ELECTROCHEMICAL CHARACTERIZATION OF *GIARDIA INTESTINALIS* CYTOCHROMES *b5*

A Thesis Submitted to the Committee on Graduate Studies in Partial Fulfillment of the Requirements for the Degree of Masters of Science in the Faculty of Arts and Science

TRENT UNIVERSITY

Peterborough, Ontario, Canada

Environmental and Life Sciences M.Sc. Graduate Program

January 2016

ABSTRACT

Electrical Characterization of *Giardia Intestinalis* Cytochromes b_5

Zhen (Alice) Yang

Giardia intestinalis is a protozoan parasite that causes waterborne diarrheal disease in animals and humans. It is an unusual eukaryote as it lacks the capacity for heme biosynthesis; nonetheless it encodes heme proteins, including three cytochrome *b*5 isotypes (gCYTB5s) of similar size. Homology modelling of their structures predicts increased heme pocket polarity compared to mammalian isotypes, which would favour the oxidized state and lower their reduction potentials ($E^{\circ\prime}$). This was confirmed by spectroelectrochemical experiments, which measured $E^{\circ\prime}$ of -171 mV, -140 mV and -157 mV for gCYTB5-I, II, III respectively, compared to +7 mV for bovine microsomal cytochrome *b5*. To explore the influence of heme pocket polarity in more detail, five gCYTB5-I mutants in which polar residues were replaced by nonpolar residues at one of three positions were investigated. While these substitutions all increased the reduction potential, replacement of a conserved tyrosine residue at position-61 with phenylalanine had the most significant effect, raising $E^{\circ\prime}$ by 106 mV. This tyrosine residue occurs in all gCYTB5s and is likely the greatest contributor to their low reduction potentials. Finally, complementary substitutions were made into a bovine microsomal cytochrome *b5 triple* mutant to lower its reduction potential. These not only lowered the $E^{\circ\prime}$ by more than 140 mV but also weakened the interaction of heme with the protein. The lower reduction potentials of the gCYTB5s may indicate that these proteins have different roles from their more well-known mammalian counterparts.

Key Words: *Giardia intestinalis*, cytochrome b_5, *b*-type cytochrome, heme protein, electron transfer protein, protozoan protein, recombinant protein, mutant protein, molecular cloning, sequence homology, spectroelectrochemistry, UV-Visible spectrophotometry

ACKNOWLEDGEMENTS

I want to thank Dr. Steven Rafferty, Dr. Barry Saville and Dr. Andrew Vreugdenhil for their expertise, time and advice on my thesis. As my supervisor, Dr. Rafferty continues to challenge and inspire me as a scientist. I want to thank him for his patience, open-mindedness and guidance.

I send my regard to all past and present members of Dr. Yee and Dr. Rafferty's lab. I want to thank Robert Pazdzior for teaching me the fine art of spectroelectrochemistry. I want to thank Guillem Dayer for keeping me out of trouble and Katie Horlock-Roberts for her kindness, warmth and delectable baked goods. I have enjoyed many interesting philosophical conversations with Adam Kemp and Danielle Drake. I also want to thank Liza Calhoun, Wendy Tseng, Megan Teghtmeyer, Kaitlyn Pinkett, Kelly Nori and Mirfath Mesbahuddin for their friendship and support. Additionally, I want to thank my "thesis support group" Marisha Lamonde, Jana Farell and Alena Celsie for their incredible support.

Finally, I want to thank my parents for their love and support. I want to thank my mom for she is my rock and always challenging me to a better version of myself. These two years have been a roller coaster ride, not to be cliché but it has been an interesting journey that helped me to mature and strengthen my critical thinking skills. I will cherish these memories, experiences and lessons for the years to come.

TABLE OF CONTENTS

LIST OF FIGURES

LIST OF TABLES

LIST OF ABBREVIATIONS AND SYMBOLS

A	Absorbance
ALA	δ-Aminolevulinic acid
ATP	Adenosine triphosphate
CYTB5A	Microsomal cytochrome b_5
CYTB5B	Mitochondrial cytochrome b_5
D	Diffusion coefficient (cm^2/s)
Δ_o	*d* orbital splitting
ε	Extinction coefficient, molar absorptivity ($M^{-1}cm^{-1}$)
E	Potential of an electrode versus a reference
***E*°**	Standard potential of an electrode or a couple
***E*°'**	Formal potential of an electrode
$E_{applied}$	Applied potential
F	Faraday constant (charge on one mole of electrons)
gCYTb5	Giardia cytochrome b_5
ΔG	Free energy
$\Delta G°$	Standard Gibb's free energy
IPTG	Isopropyl-β-D-thiogalactoside
kDa	Kilo Dalton
l	Path length of cuvette in spectrometry
n	Number of electrons transferred
NADH	Nicotinamide adenine dinucleotide
OTTLE	Optically transparent thin-layer electrode
PMSF	Phenylmethanesulfonylfluoride
R	Universal gas constant ($8.314\ J \bullet mol^{-1} \bullet degree^{-1}$)
SDS-PAGE	Sodium dodecyl sulfate polyacrylamide gel electrophoresis
SEC	spectroelectrochemistry
SHE	Standard hydrogen electrode
δ	Largest distance a molecule has to travel to the nearest electrode surface
T	Absolute temperature in Kelvin (*K*)
τ	Equilibrium time
TCEP	Tris(2-carboxyethyl)phosphine
μ	Ionic strength
UV-Vis	Ultraviolet-visible

INTRODUCTION

1. Overview

Giardia intestinalis is an anaerobic protozoan parasite that occupies the upper small intestine of mammals, birds and reptiles. Due to its parasitic lifestyle, many biochemical pathways usually present in aerobes are absent. Giardia lacks mitochondria and the associated heme proteins for cytochrome-mediated electron transfer, as well as the capacity to synthesize heme. While Giardia was long thought not to have heme proteins, in 2007 genomic analysis showed the presence of genes for four cytochrome b_5 isotypes. These electron transfer proteins have well-known roles in supplying electrons to heme-based monooxygenases, fatty acid desaturases and the mitochondrial respiratory chain, but their roles in Giardia are unknown. Homology models of their structures suggest that their electrochemical properties differ significantly from more well-known family members, which may indicate completely different roles for these proteins in Giardia. The electrochemical properties of three of the Giardia isotypes plus several active-site mutants of Giardia cytochrome b_5 isotype-I (gCYTB5-I) are the subject of this work.

2. Biology and biochemistry of *Giardia intestinalis*

The protozoan *Giardia intestinalis* is an aerotolerant anaerobic parasite that attaches to the epithelial cells in the upper small intestine of mammals, birds and reptiles. Infection begins when Giardia cysts from contaminated water, food or fecal-oral contact are ingested. The acidic environment of the host's stomach triggers excystation and the formation of flagellated, binucleate trophozoites, which adhere to the epithelial cells of the upper small intestine where they reproduce by asexual binary fission (Figure 1). As

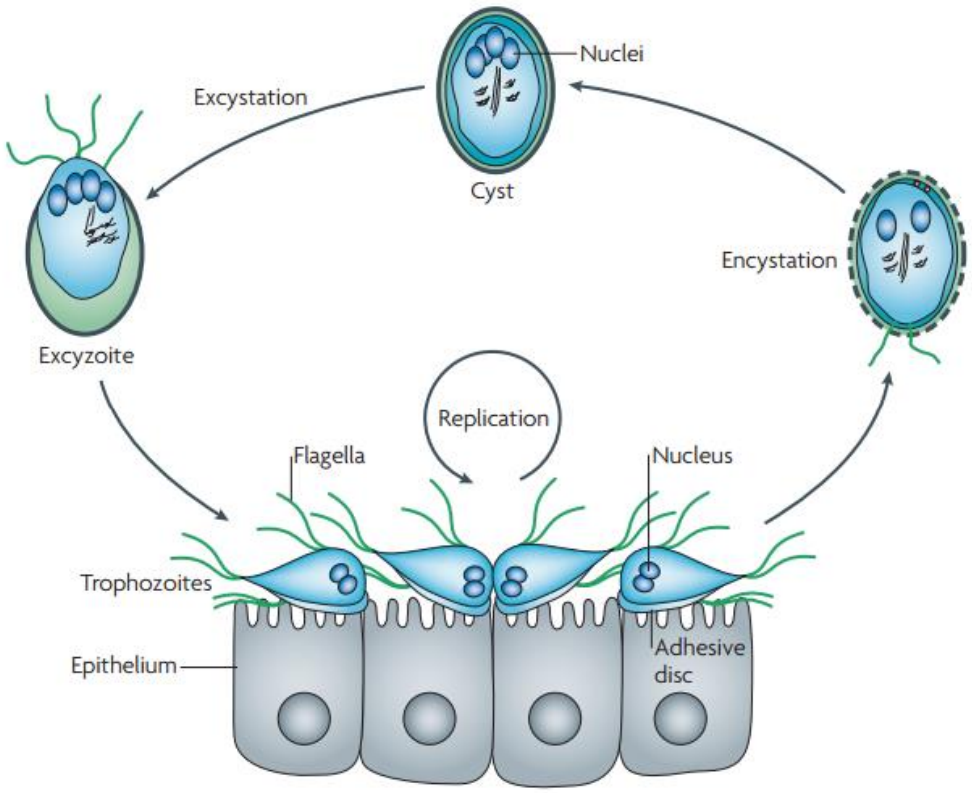

Figure 1. Life cycle of *Giardia intestinalis*. Infectious cysts from the environment enter into the gastrointestinal tract of the host via ingestion. The acidic environment of the stomach triggers excystation into the trophozoite form and attachment to the small intestine, where trophozoites replicate by binary fission. Giardia is then excreted in the cyst form to complete the infectious cycle (Ankarklev, Jerlstrom-Hultqvist et al. 2010).

trophozoites pass through the intestinal tract, they convert to cysts, which are excreted with the feces to become the source for new infections. Giardia infection is one of the most common causes of infectious diarrhea, known as giardiasis (Savioli, Smith et al. 2006).

Although it is a eukaryote, Giardia does not use oxygen for ATP production. Most eukaryotes use aerobic respiration to produce the energy currency ATP, the components of which are glycolysis, the citric acid cycle and oxidative phosphorylation. Oxidative phosphorylation occurs in the mitochondria and its respiratory chain makes use of soluble and membrane-bound cytochromes, which are electron transfer proteins that possess the iron-containing cofactor heme. Giardia is unusual among eukaryotes as it lacks

mitochondria, and does not have all the enzymes of the citric acid cycle, thus oxidative phosphorylation is absent (Lindmark 1980, Jian Han 2012). Instead, Giardia uses substrate-level phosphorylation (such as glycolysis) and pyrophosphate for ATP production (Brown, Upcroft et al. 1998). Besides lacking respiratory heme-complexes, Giardia also lacks other common heme proteins such as catalase, peroxidases, oxidases, and monooxygenases. Moreover the Giardia genome encodes none of the genes for heme biosynthesis, a pathway that is nearly universal among eukaryotes and prokaryotes. Surprisingly, its genome does encode heme proteins, including one flavohemoglobin and four members of the cytochrome b_5 family (Morrison, McArthur et al. 2007, Rafferty, Luu et al. 2010, Alam, Yee et al. 2012).

3. Heme and heme proteins

Heme is a coordination complex between iron (usually in the +2 or +3 oxidation states) and the protoporphyrin IX macrocycle, which provides four nitrogen atoms as ligands (electron pair donors) to the metal cation (Figure 2). Protein-heme coordination complexes are either five- or six-coordinate, with approximately square pyramidal or octahedral coordination complex geometries, respectively. Octahedral complexes (six-coordinate) are of particular importance for this study. In such complexes the iron is coordinated by the four nitrogen atoms from the porphyrin ring and two axial ligands perpendicular to the plane of the heme. In many cytochromes these axial ligands are a pair of histidine residues. Due to electron-electron repulsion between ligand and metal orbitals, the five *d* orbitals of the iron can be split into two different energy levels, such

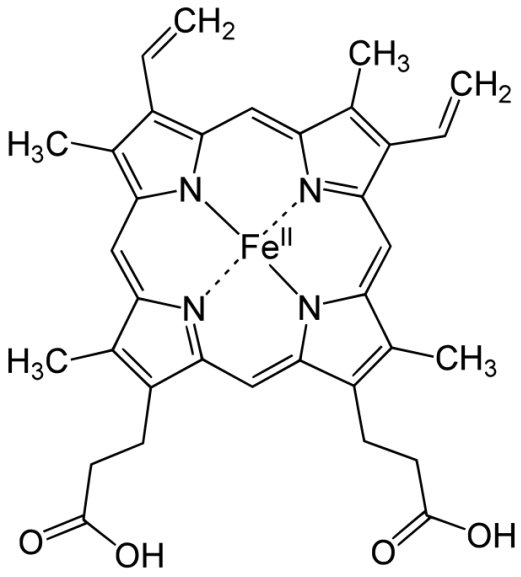

Figure 2. Structure of heme b. Protoporphyrin IX is ligated to an iron ion that cycles between Fe (II) and Fe (III) oxidation states (Walker, Emrick et al. 1988).

that d_z^2 and d_x^2-$_y^2$ orbitals rise in energy, while the other three orbitals of d_{xz}, d_{xy}, and d_{yz}, are lower in energy (Figure 3). Strong field ligands cause a large energy difference in octahedral *d* orbital splitting, Δ_o. If the energy difference between d_z^2, d_x^2-$_y^2$ (high energy) and d_{xz}, d_{xy}, and d_{yz} orbitals (low energy) is large compared to the energy to pair electrons in the same orbital, electrons will fill the lower energy *d* orbitals first (two electrons per orbital). This arrangement is classified as low spin because there is a minimal number of unpaired electrons (Figure 3). Alternatively, weak field ligands cause only small changes in the energy difference of the *d* orbitals, leading to a small Δ_o (Figure 3). In such a case with a small energy difference between d_z^2, d_x^2-$_y^2$ (high energy) and d_{xz}, d_{xy}, and d_{yz} orbitals (low energy), the energy of pairing two electrons in the same orbital exceeds the splitting energy, and the electrons will begin to occupy the higher energy *d* orbitals before they begin to pair. This arrangement is classified as high spin (Figure 3). Certain heme proteins such

as cytochromes exist in one spin state, usually low spin, regardless of the oxidation state, which facilitates rapid electron transfer. In others, such as the oxygen-binding globins, spin-state changes are coupled with conformational changes in the protein which promote cooperative binding of O_2. Control of heme oxidation state and spin state is the basis for how the same cofactor can be used by different proteins for wide range of biological roles.

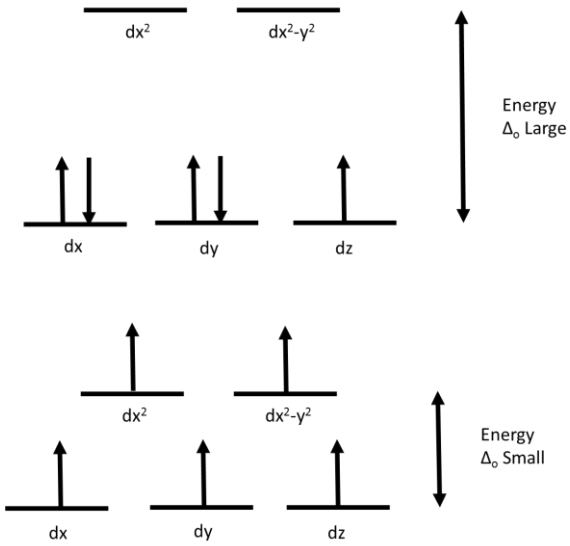

Figure 3. **The electron arrangement of d orbitals in octahedral geometry.** The low spin (top) and high spin (bottom) of d orbital splitting in sixth coordinate octahedral complex geometry

Heme is a useful cofactor in many biological processes and it can be made by most organisms in a highly conserved biosynthetic pathway. In the overwhelming majority of eukaryotes, heme synthesis starts in the mitochondrial matrix from δ-aminolevulinic acid, which is transported into the cytosol to form coproporphyrinogen III which is transported back into the mitochondria to become heme in a highly conserved process (Ajioka, Phillips et al. 2006). Nearly all eukaryotes use heme, including several that cannot synthesize it, such as the nematode *Caenorhabditis elegans* and the parasitic protists *Giardia*, *Entamoeba*, *Cryptosporidium*, *Blastocystis*, and *Trichomonas* (Pyrih, Harant et al. 2014).

4. Cytochromes and their roles in electron transfer

Cytochromes are heme proteins that are functionally defined by their use of this cofactor solely for electron transfer. Within this functional definition there are many different and separate structural classes of cytochromes, including soluble and membrane-bound proteins. In all cytochromes the heme iron cycles between oxidized (Fe^{3+}) and reduced (Fe^{2+}) states.

Electron transfer, the movement of an electron from one molecule (the electron donor) to another (the electron acceptor) is essential to many biochemical pathways. To be biologically useful electron transfer must be both rapid and specific. Electron transfer mechanisms in which both donor and acceptor are transition metal coordination complexes (such as cytochromes) are classified as two types: inner sphere and outer sphere (Eyring 1935). Inner sphere electron transfer proceeds through an intermediate in which the donor and acceptor coordination complexes share a ligand. As this requires coordination bond breakage and reformation, this process can be slow. In contrast, outer sphere electron transfer occurs without ligand substitution in either the donor or acceptor and is faster. It is likely on this account that all examples of biological electron transfer occur by the outer sphere mechanism. Rapid electron transfer also requires that the distance between donor and acceptor be short. As distance increases, the rate of electron transfer exponentially decreases (Sigel 1991). Usually the distance between donor and acceptor metal centres is on the order of 10 Å. Other factors that influence electron transfer rate include the nature of intervening media between donor and acceptor, their relative orientation, and the conformational differences between the oxidized and reduced state of each participant. Rapid transfer is favored when these conformational differences in the oxidized and reduced states are small (Lippard and Berg 1994). Biological electron transfer also requires

specificity between donor and acceptor and for this reason it occurs through specific protein-protein complexes in which the donor and acceptor dock prior to actual electron transfer.

The cytochrome class that is the focus of this thesis is cytochrome b_5. Cytochrome b_5 has been found in bacteria, fungi, animals and plants (Jagow 1980). The most well-studied member of this class is microsomal cytochrome b_5 (CYTB5A), which is anchored to the endoplasmic reticulum by a carboxyl-terminal hydrophobic alpha helix and participates in several important processes. One reaction is fatty acid desaturation, in which cytochrome b_5 receives an electron from NADH-cytochrome b_5 reductase and donates it to fatty acyl desaturases (Figure 4). Fatty acids serve a structural role in the formation of phospholipids and cellular membranes, whose fluidity is determined by the extent of acyl chain unsaturation. Fatty acids also serve as precursors for polyunsaturated fatty acids such as arachidonic acid that are precursors to signalling molecules such as prostaglandins, thromboxanes, and leukotrienes which mediate and regulate many cellular functions. CYTB5A is also involved in sterol biosynthesis, donating an electron to methyl sterol oxidase that oxidizes the C-30 methyl group of lanosterol, a cholesterol precursor (Vergeres and Waskell 1995).

Another major role of CYTB5A is as a participant in cytochrome P450-catalyzed monooxygenation reactions. In spite of their name cytochrome P450s are not electron transfer proteins but are redox enzymes that bind and activate molecular oxygen, O_2, for insertion of an oxygen atom into a substrate, with the other oxygen atom being reduced to H_2O. Substrates of cytochromes P450 include endogenous and exogenous compounds, such as fatty acids, steroid hormones, vitamin D_3, xenobiotics, pharmaceuticals and toxic compounds. CYTB5A is an electron donor to many cytochrome P450 enzymes, and it can

also modulate activity without electron transfer by forming a complex with the enzyme to increase its oxidation efficiency (Vergeres and Waskell 1995).

A soluble, alternative splice variant of CYTB5A that lacks the C-terminal membrane anchor is found in red blood cells. It mediates electron transfer from NAD(P)H oxidoreductase to methemoglobin, in which the heme cofactor is in the ferric state and is unable to bind oxygen (Petragnani, Nogueira et al. 1959). The combination of the reductase and CYTB5A restores methemoglobin to its functional state.

The other major cytochrome b_5 found in mammals is mitochondrial cytochrome b_5 (CYTB5B), which is anchored to the mitochondrial outer membrane. Unlike microsomal cytochrome b_5, little is known about the mitochondrial isotype. CYTB5B also interacts with mitochondrial cytochrome P450 either to transfer a second electron or induce conformational changes in the P450 enzyme upon formation of the CYTB5B-cytochrome P450 complex (Ogishima, Kinoshita et al. 2003). Additionally, CYTB5B and its reductase are involved in detoxification reactions through reduction of N-hydroxylated compounds, such as amidoxime, in association with a molybdenum enzyme, known as mitochondrial amidoxime reducing component (mARC) (Ito, Hayashi et al. 1981).

Finally, cytochrome b_5 can be a domain within multi-domain proteins that also contain redox-active flavin cofactors and binding sites for electron donors such as nicotinamide adenine dinucleotide (NADH). Examples of such fusion enzymes include flavocytochrome b_2, sulfite oxidase (Guiard and Lederer 1977), and NADH cytochrome b_5 oxidoreductase (Deng, Parthasarathy et al. 2010).

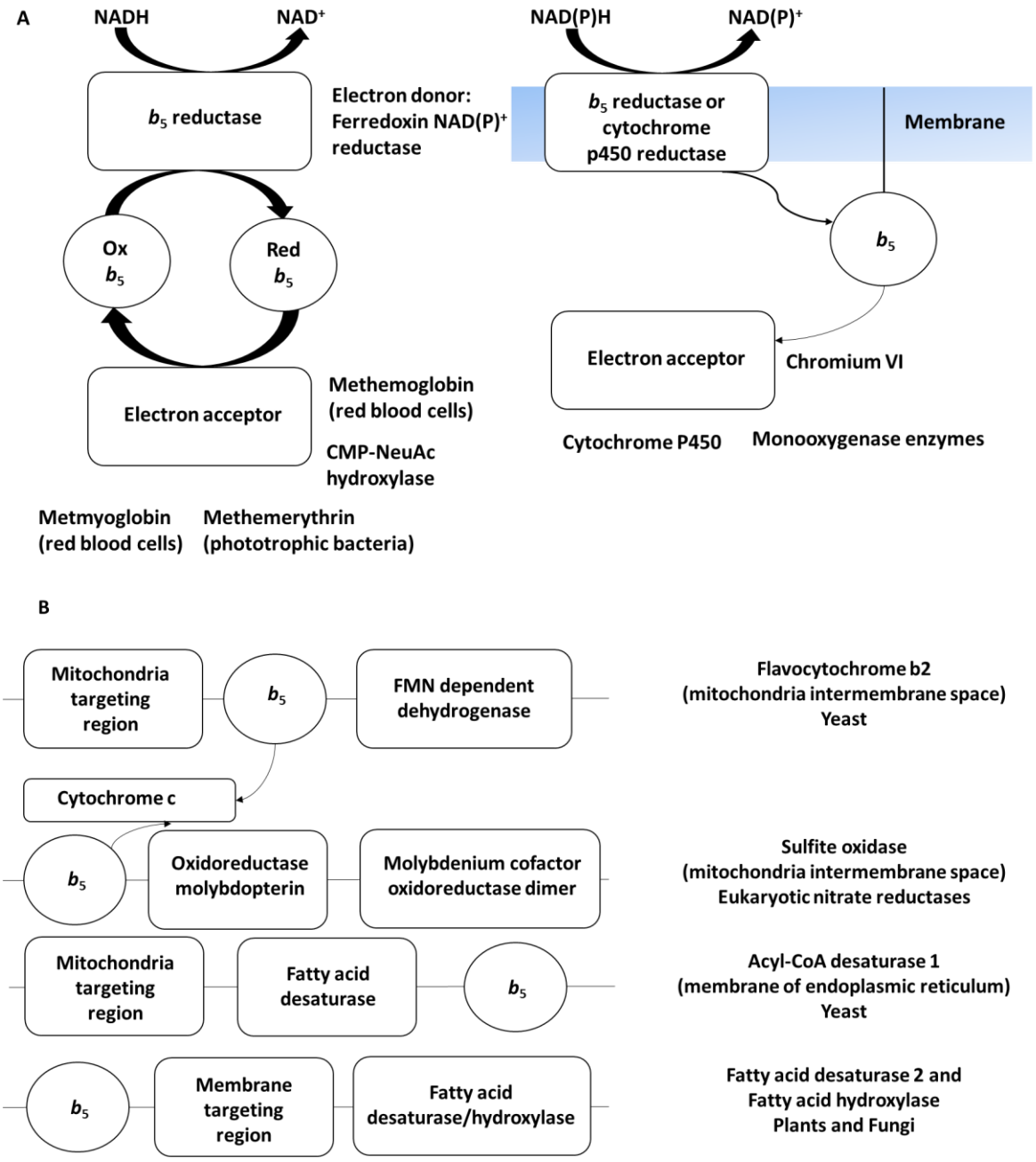

Figure 4. (A) **Roles of cytochrome *b*$_5$**: Soluble (left) and membrane-bound (right) cytochromes b_5 act as electron shuttles accepting electrons from reductase and donating them to oxygen atom of various oxygenases. However, these reducing and oxidizing partners are not found in gCYT*b*5, thus the protein's role in *Giardia intestinalis* is unknown. (B) Cytochrome b_5 as a subunit of other proteins (Alam 2014)

5. Structure of cytochrome b_5

Although the level of amino acid sequence identity across the cytochrome b_5 class may be 30% or less, the protein fold as determined experimentally by both NMR and X-ray diffraction is highly conserved. The structure of microsomal cytochrome b_5 is the most well-characterized member of this class (Figure 5). CYTB5A is a small acidic protein (MW 15.2 kDa-16.7 kDa) and it consists of a single polypeptide chain of 131 to 146 amino acid residues (Sergeev, Gilep et al. 2006). The protein folds into 6 α helices, 5 β sheets and various β turns and has two functional domains: a soluble heme-binding amino terminal domain (~90 residues) and a short hydrophobic carboxyl-terminal α-helix (~14-18 residues). The C-terminal domain targets and anchors cytochrome b_5 to the membrane of mitochondria and endoplasmic reticulum. The N-terminal domain extends out of the membrane and participates in electron transfer reactions. The C-terminal α-helix is connected to the N-terminal domain *via* a proline-containing hinge/linker region of 7 to 15 residues followed by seven hydrophilic residues at the C-terminus that is exposed to the cytosol and encodes a post-translational membrane-targeting region (Schenkman and Jansson 2003). The presence of positively-charge amino acids in this region directs the protein to the outer mitochondrial membrane, whereas their absence targets the protein to the endoplasmic reticulum (Mitoma and Ito 1992). The membrane anchor of cytochrome b_5 can be removed by limited proteolysis (Reid and Mauk 1982) or recombinant expression (Funk, Lo et al. 1990), resulting in soluble protein.

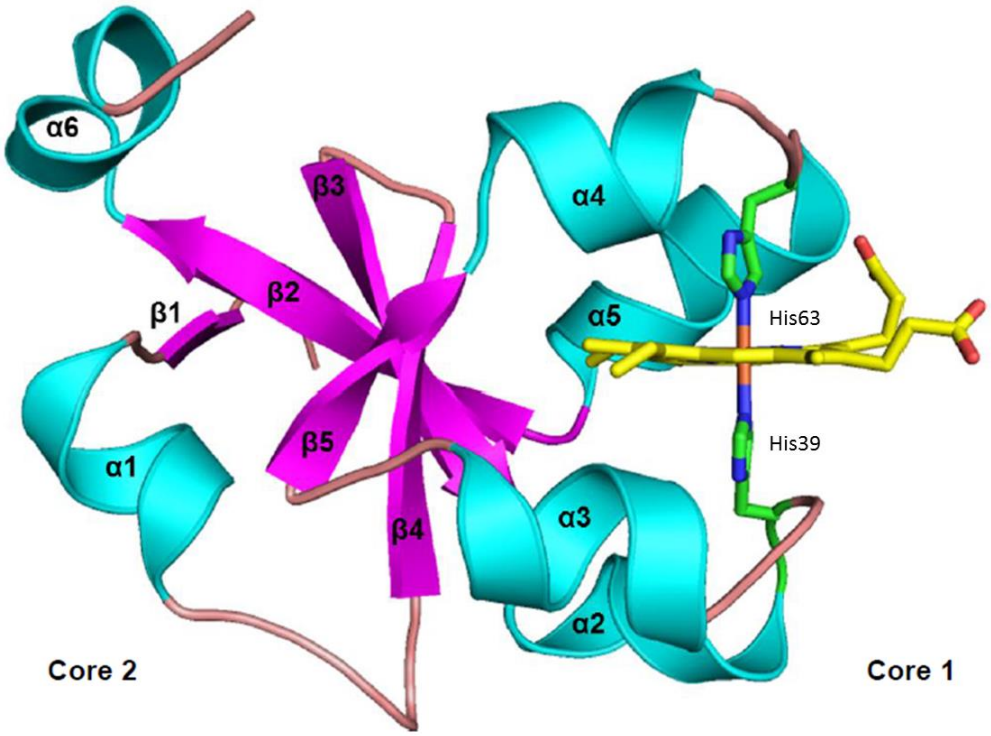

Figure 5. Structure of bovine microsomal cytochrome *b*$_5$ CYTB5A (1cyo.pdb). Alpha-helices are shown as cyan ribbons, beta strands as magenta arrows and loops are salmon. The heme and the two histidine axial (histidine-63 and histidine-39) ligands are shown in yellow and green ball and stick model (Mathews, Levine et al. 1971).

The secondary structure of the heme-binding domain from N-terminus to C-terminus is β1-α1-β4-β3-α2-α3-β5-α4-α5-β2-α6, which forms two hydrophobic cores on either side of a curved β sheet (Figure 5). The large hydrophobic core 1 binds heme (α2-α5), while the smaller core 2 in the shape of a barrel (β1-β4, α1 and α6) stabilizes core 1. Core 1 forms a hydrophobic crevice of α-helices connected by a turn (Lederer 1994). Inside core 1, the heme cofactor is coordinated by the ε-nitrogen of two conserved histidine residues (His39 and His63) as the fifth and sixth axial ligands. Overall, the iron has a six-coordinate geometry with an octahedral arrangement of ligands. The iron bound to the heme can be in the oxidized state (Fe^{3+}) or gain an electron to become the reduced (Fe^{2+})

state. As the deprotonated protoporphyrin IX ring has a charge of -2, in its metal-binding state, heme alternates between a net charge of +1 (oxidized, Fe^{3+}) and 0 (reduced, Fe^{2+}). The His39 residue lies within a highly conserved sequence motif (HPGG) between the α2 and α3 helices, while His63 residue is located within the VGHS loop motif between helices α4 and α5, which is usually preceded by a pair of acidic residues (glutamic acid or aspartic acid) (Mathews, Levine et al. 1971). The axial histidine ligands are strong field ligands that do not allow spin state changes and so the iron is low spin in both Fe (II) and Fe (III) oxidation states. The heme group is oriented such that the two vinyl groups are buried, with one propionate group exposed to the solvent and the other bound to the surface of the protein.

The heme-binding pocket is lined with hydrophobic residues which help to stabilize the reduced state. The aromatic ring of Phe58 interacts with the imidazole ring of His63 through π-stacking interactions and with the porphyrin ring through T stacking interactions (Shan, Lu et al. 2005). Leu23, Phe35, and Leu46 make contact with the porphyrin ring, while Tyr30, Leu36 and Phe74 are more distant but are still a part of the heme core (Lederer 1994, Smith, Kahraman et al. 2010) (Figure 6).

Based on sequence comparisons there are three main groups of cytochrome b_5. Group I represents canonical cytochrome b_5 typically containing a C-terminal hydrophobic tail and it includes both CYTB5A and CYTB5B. Group II members lack a C-tail anchor and possess an N-terminal extension of approximately 10 to 50 amino acids. Group III represents cytochrome b_5 lacking in both N- and C- terminal extensions (Figure 7) (Pyrih, Harant et al. 2014).

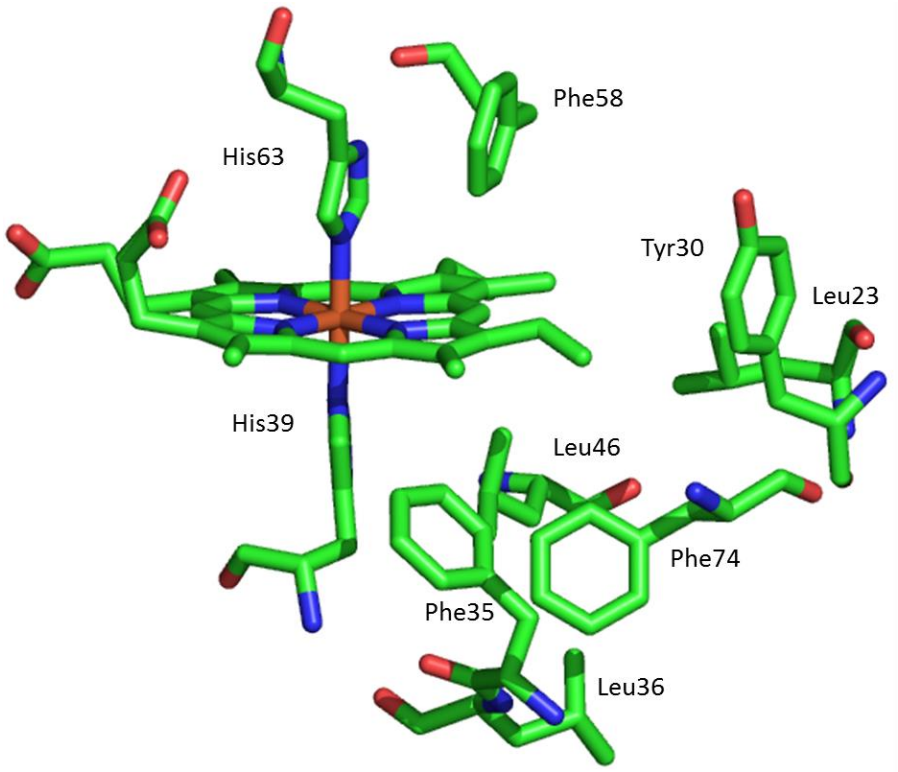

Figure 6. The heme-binding site of bovine microsomal cytochrome b_5. The heme binding site of bovine b_5 is mostly lined with non-polar amino acid residues. The solvent-exposed heme edge is on the left

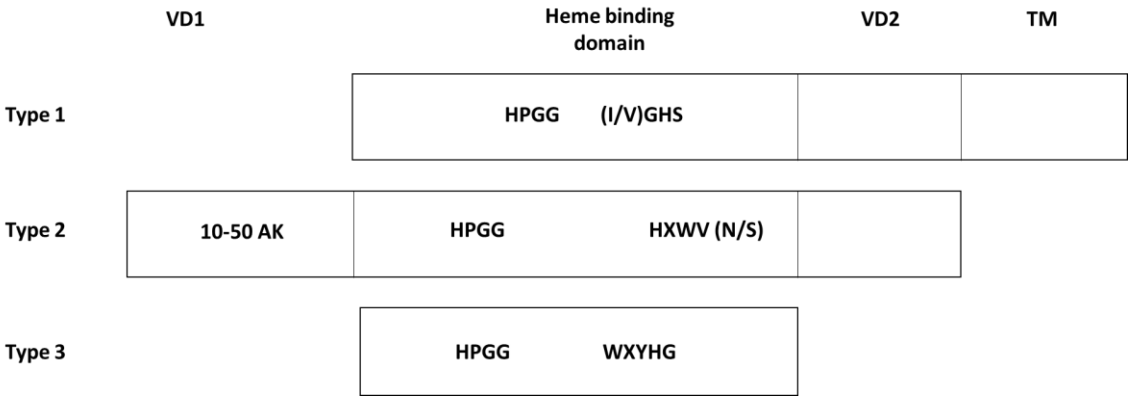

Figure 7. The three groups of cytochrome b_5. Diagram of the structural difference between group I, II and III cytochromes b_5. VD1 (amino-terninal variable domain I) ; VD2, (carboxy-terminal variable domain II) . TM, transmembrane anchor. Giardia cytochromes b_5 belong to type II (Pyrih, Harant et al. 2014).

6. Spectroscopic properties of cytochromes b_5

As heme proteins, cytochromes b_5 have characteristic ultraviolet-visible (UV-vis) spectra. UV-vis spectroscopy records electronic transitions of a chromophore that occur in the ultraviolet (180 -400 nm) and visible (400-700 nm) regions of the spectrum. The absorption at specific wavelengths indicates electronic transitions in a molecule due to excitation of an electron from a lower energy state to a higher energy state. Absorption in the UV region corresponds to higher energy transitions than absorption in the visible region. Aromatic compounds absorb between 250 to 450 nm due to $\pi \rightarrow \pi^*$ transitions of electrons in the aromatic ring. Since most proteins contain aromatic amino acids (phenylalanine, tryptophan, and tyrosine), their absorption occurs near 280 nm. Heme proteins such as cytochrome b_5 have additional bands in their spectra resulting from the heme cofactor. The porphyrin ring of heme is aromatic and has extensive delocalization of π-orbital electrons, whose $\pi \rightarrow \pi^*$ transitions result in an intense Soret (γ) band between 380 and 450 nm, and weaker alpha (α) and beta (β) bands in the visible region between 520 and 570 nm. The position of these absorbance bands is sensitive to oxidation, coordination and spin state of the heme iron, and the local heme environment (Holler, Skoog et al. 2007). In the oxidized state (Fe^{3+}), cytochromes b_5 have a strong Soret bands near 412nm and weak broad absorption in the visible region (500-650 nm). In the reduced state (Fe^{2+}), the Soret band shifts to ~ 420 nm and pronounced α and β bands appear in near 560 nm and 530 nm respectively in the visible region (Figure 8).

Owing to these properties the heme content of a protein can be quantified by UV-visible spectroscopy. When treated with alkaline pyridine, heme proteins unfold and the

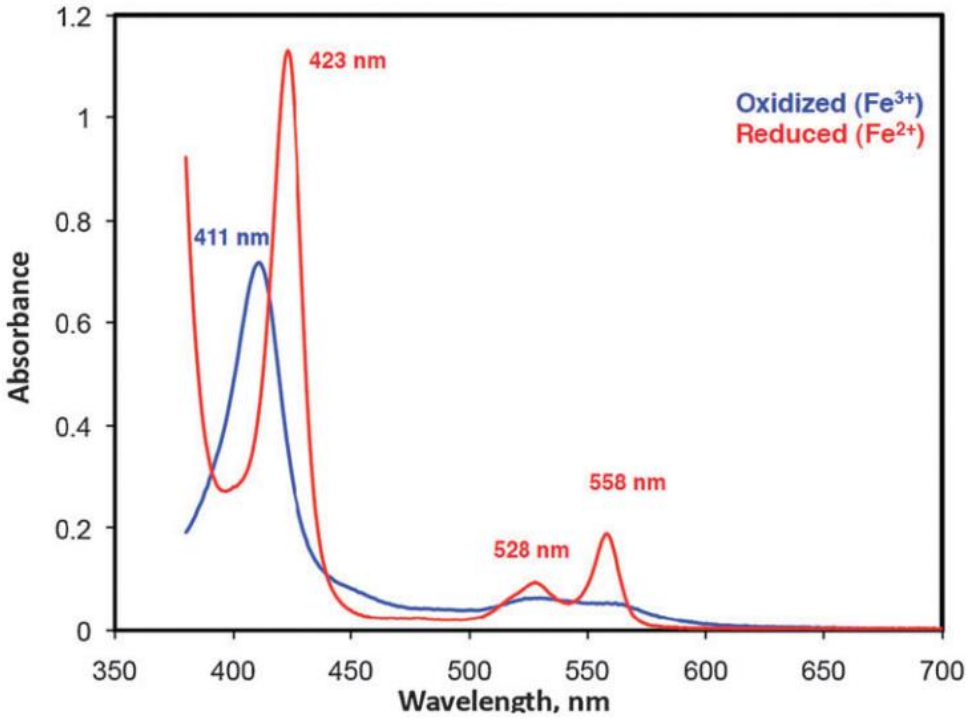

Figure 8. Visible absorption spectrum of cytochrome *b*$_5$ isotype I from *Giardia lamblia*, as obtained by Alam et al. 2013. The oxidized protein (blue) shows a Soret band at 411 nm, which shifts to 423 nm in the reduced state (red). In addition there are two visible peaks at 528 and 558nm in the reduced state.

free heme forms a complex with two pyridine molecules as axial ligands. The reduced heme-pyridine complex has an extinction coefficient of 22.1 $mM^{-1}cm^{-1}$ for the difference in absorbance at A_{556} (peak) – A_{520} (trough). This pyridine hemochrome assay provides a means to measure the fraction of purified protein that has heme bound to it, as the heme content of heme proteins is often stoichiometric (Paul, Theorell et al. 1953).

7. Structure and characteristics of Giardia cytochromes *b*$_5$

Giardia cytochrome *b*$_5$ isotypes I, II and III (gCYTB5s) are group II soluble cytosolic proteins that lack a carboxyl terminal transmembrane anchor (Pyrih, Harant et al. 2014). The UV-visible spectra of gCYTB5s in both oxidation states are similar to other

family members. The three Giardia cytochrome b_5 genes possess the invariant coordinating histidine residues and have 25 to 40% sequence identity to other members of this protein family; among the gCYTB5s the level of amino acid identity is 36-41% . However, unlike the well-characterized mammalian cytochromes b_5 the functions of the gCYTB5s are currently unknown. Bioinformatic screening of the Giardia genome has identified only one possible electron donor and no known electron acceptors. This suggests that Giardia may use gCYTB5s for different roles, which could reveal more about metabolic pathways in Giardia.

No Giardia cytochrome b_5 structures have been determined experimentally to date, however structures have been obtained by homology modelling using the cytochrome b_5 domain of human NADH cytochrome b_5 oxidoreductase 4 (CYB5R4, 3lf5.pdb) as a template, which has about 34% sequence identity to each of the Giardia proteins. The template and the gCYTB5s share the following: the pair of axial histidines (His65, His88; numbered according to gCYTB5-I) in the helix-loop-helix motif; certain heme pocket residues (Tyr61, Pro66, Val91); and certain residues of the β-sheet platform on which the heme-binding α-helices are supported (Trp48, Gly53, Val55, Tyr56, and Gly103). While gCYTB5-II has the first coordinating histidine within the conserved HPGG motif, isotypes I and III are among the few cytochromes where the highly conserved HPGG loop motif is altered, to HPAG (Figure 9). The substitution of glycine to alanine could result in loss of conformational flexibility in the protein backbone, but also have unique structural and functional implications due to proximity to the histidine ligand and heme. In addition, the second VGHS loop motif varies among the Giardia isotypes and lacks the acidic residues that usually precede it. Furthermore, within the heme-binding pocket the gCYTB5s have

small hydrophilic residues (cysteine, alanine and threonine for gCYTB5-I, II, and III respectively) rather than a phenylalanine residue (CYTB5A position Phe58) that is conserved in most mammalian cytochromes (Figure 9). In bovine microsomal b_5, this residue stacks with the imidazole ring of histidine 63 in a parallel π-stacking mode and with the porphyrin ring in a T-stacking mode (Shan, Lu et al. 2005). On the opposite side of the heme the Giardia isotypes all have a tyrosine substituting for phenylalanine (CYTB5A position Phe35). The hydroxyl group on tyrosine can help to stabilize charge on the iron by ion-dipole interactions. Overall, the heme-binding domains of gCYTB5s are more hydrophilic compared to other members of the cytochrome b_5 family, such as CYTB5A and CYTB5B.

Furthermore the Giardia cytochrome b_5 isotypes have fewer acidic residues on the face of the protein containing the exposed heme edge compared to bovine microsomal cytochrome b_5 (Figure 10). These negatively charged amino acids form complementary electrostatic interactions with positively charged basic residues on redox partners, such as cytochrome P450 and cytochrome *c*. The lack of acidic residues may affect the nature of the interaction of gCYTB5s with their redox partners, as complementary charge interactions between the surface acidic residues of CYTB5A and CYTB5B with surface basic residues on their partners are critical for productive docking of these proteins in orientations that promote rapid electron transfer (Deng, Parthasarathy et al. 2010).

```
bmCYTb5          AVKYYTLEEIQKHNNSKSTWLILHYKVYDLTKFLEEHPGGEEVLREQAGGDATENFEDVG
gCYTb5-I         ---NYTANQVYEHRSEDDCWVTYRGRVYDITQYLDWHPAGKDILRPFFGYDITEACNVAH
gCYTb5-II        ---FYTPEEIASHASMDDAWMSYRGKVYDITHYVRYHPGGLQCMQEYMGKDMTHAADSVH
gCYTb5-III       ---PITPEEVLRHRDVNDCWVSHKGIVYNLTPYLRYHPAGIAPIEDYYGYDITAVTAAVH
                      * :::  * . .. *:  :  **::* ::  **.*   :.   * * *     .

bmCYTb5          HSTDARELSKTFIIGELHPDDRS
gCYTb5-I         SWVGIHKMIEPLHIGMLQGP---
gCYTb5-II        KWVNVATMLRPLAIGTVKTH---
gCYTb5-III       GFVQVEQIIAPLAVGVLNGD---
                   .    :   : :* :.
```

Figure 9. Sequence alignment of bovine microsomal b_5 and Giardia cytochromes b_5. The highlighted yellow sequences represent the conserved motifs around the axial histidine ligands. The highlighted green residues are the sites that were mutated in this work. "*" and ":" indicates positions where the aligned sequences have identical and conserved residues, respectively.

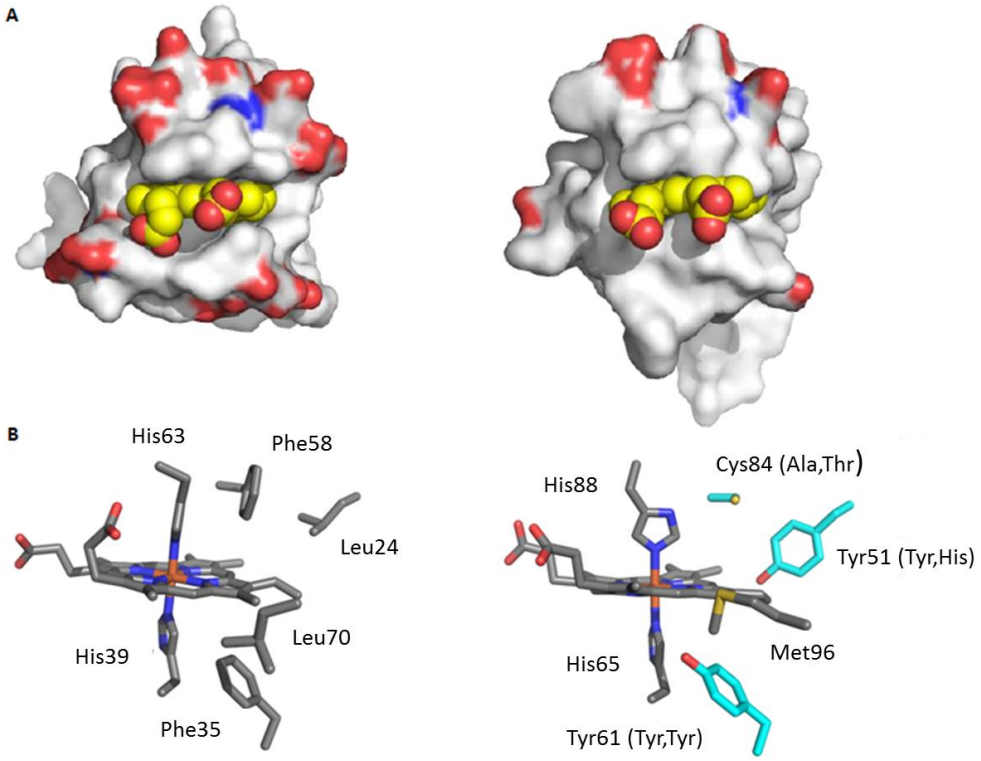

Figure 10. Structural differences between microsomal cytochrome b_5 and gCYTB5-I. A) Surface charge distribution of acidic residues (red) on microsomal cytochrome b_5 (left) and the model of gCYT*b5*-I (right). B) Heme binding sites of bovine microsomal cytochrome b_5 (left, 1cyo.pdb) and gCYTb5-I (right, homology model with 3lf5.pdb as the template). The amino acid residue of gCYT*b5*-II and III are indicated in brackets respectively. Nonpolar residues are in grey, polar residues cyan. The imidazole rings of the coordinating histidine residues are nearly coplanar in bovine microsomal cytochrome b_5 and nearly perpendicular in gCYTb5-I. These images were prepared using PyMOL (Schrödinger, NY) (Alam 2014).

While reduction potentials for other known cytochromes b_5 range from +78 mV to -100 mV *vs* SHE, the reduction potential of gCYTB5-I, the only example of a Giardia cytochrome whose reduction potential has been measured is much lower. gCYTB5-I has a reduction potential of -165±7 mV compared to +5 mV for bovine CYTB5A (Table 1) (Alam, Yee et al. 2012). The charge on heme in the oxidized state is +1 (the sum of the Fe^{3+} charge and the porphyrin dianion charge of -2). This can be stabilized by nearby hydrophilic or negatively charged amino acid residues by ion-dipole and electrostatic interactions, respectively. Since the heme-binding pockets of gCYTB5s predicted by homology model structures are more hydrophilic compared to bovine microsomal cytochrome b_5, it is possible that these hydrophilic residues help to stabilize the oxidized iron and lower the reduction potential.

Table 1. Reduction potentials of members of the cytochrome b_5 family (Alam, Yee et al. 2012)

Protein	$E^{\circ\prime}$ (mV *vs*. SHE)
gCYTb5-I (this work)	-165^a
Bovine liver, microsomal[32]	$+5^b$
Tetrahymena, microsomal[33]	-42^c
Yeast flavocytochrome b_2[34]	-31^c
Rat liver, mitochondrial outer membrane[30]	-102 to $+40^a$
Rat liver, mitochondrial outer membrane[30]	-102^b
Ascaris suum, cytosolic[24]	$+78^c$
Human (liver)[35]	-3^c
Human (erythrocyte)[36]	-9^a

[a] Cyclic voltammetry. [b] Optically transparent thin layer electrode. [c] Potentiometric titration.

8. Electrochemistry

When a molecule loses an electron, it becomes oxidized and when a molecule gains an electron, it becomes reduced. As free electrons do not exist in chemical systems, oxidation of one molecule (the electron donor) must be paired with the reduction of another (the electron acceptor). The reduction potential of a redox pair, such as the oxidized and reduced states of a cytochrome, is a measure of the free energy change associated with the change in oxidation state relative to that of a reference redox pair, usually the standard hydrogen electrode (SHE), which is assigned a reference value of 0 mV. Compared to this reference, a reaction with a positive reduction potential favours the reduced state and a reaction with negative reduction potential favours the oxidized state.

Since reduction potential is a relative term, it is measured as the energy difference between two reactions. This is accomplished using a working electrode and a reference electrode (Figure 11). The electron transfer occurs at the working electrode while the reference electrode maintains a constant potential under different experimental conditions. While the standard hydrogen electrode (SHE) is the most common reference electrode to which potentials are measured it is rarely used in practice, as it is cumbersome to work with gaseous hydrogen. Instead, several other references are used that are more compact, practical, and commercially available. These include the saturated calomel electrode ($E°$=+241 mV vs SHE in saturated KCl) and the silver chloride electrode ($E°$=+197 mV vs SHE in saturated KCl). The reaction of interest occurs in another cell linked to the reference electrode by a salt bridge consisting of a porous frit in contact with each half-cell's electrolyte that allow electrical contact yet minimizes diffusion between the two half-cells.

The cell reaction of two redox species, A and B, would be:

$$A_{oxidized} + B_{reduced} \rightleftharpoons A_{reduced} + B_{oxidized} \quad (1)$$

The half-reaction for a given species, "A", in its half-cell in the reduced form by convention would be as follows:

$$A_{oxidized} + e^{-} \rightleftharpoons A_{reduced} \quad (2)$$

The Gibb's free energy for this equilibrium reaction in terms of concentration of oxidized and reduced species is as follows:

$$\Delta G = \Delta G° + (nRT)\ln\frac{[oxidized]}{[reduced]} \quad (3)$$

Where $\Delta G°$ is standard Gibb's free energy change (J/mol), R is the universal gas constant (8.314 J•mol^{-1}•degree^{-1}) and T is the absolute temperature in Kelvin (K). The Gibb's free energy change of the oxidation-reduction equilibrium is related to the cell potential by Faraday's equation:

$$\Delta G = -nFE \quad (4)$$

Where E is the electrode potential (volts, V), n is the number of electrons transferred in the reaction and F is the charge on a mole of electrons (the Faraday constant, 96 487 Coulombs•mol^{-1}).

Under standard state conditions with the reactants and products at 1 M activity, the standard Gibb's free energy can be written as:

$$\Delta G° = -nFE° \quad (5)$$

$E°$ is the standard electrode potential in volts or millivolts at which all components are present at 1 M activity. The standard reduction potential is the electrical potential at which the concentrations of the oxidized and reduced species are equivalent. A reaction is

spontaneous when $\Delta G°$ is negative, which occurs when the cell potential is positive.

The applied potential of the working electrode is related to the concentration of the reduced and oxidized species by the Nernst equation:

$$E_{cell} = E° - \frac{RT}{nF} \ln \frac{[\mathrm{A}_{\mathrm{reduced}}][\mathrm{B}_{\mathrm{reduced}}]}{[\mathrm{B}_{\mathrm{oxidized}}][\mathrm{A}_{\mathrm{oxidized}}]} \quad (6)$$

Where A refers to the half-reaction of interest and B to the half-reaction of the reference cell. Assuming 0 Volts with respect to the reference reaction simplifies the Nernst equation to:

$$E_{\mathrm{half\ cell}} = E° + \frac{RT}{nF} \ln \frac{[\mathrm{A}_{\mathrm{oxidized}}]}{[\mathrm{A}_{\mathrm{reduced}}]} \quad (7)$$

A standard state in which all species have an activity of 1 is not practical for biological reactions as this would imply a pH of zero ($[H^+]$ = 1 M). Instead the biochemical standard state is used, which assumes a physiological pH (usually 7, unless defined otherwise) and ionic strength (often 0.1 or 0.15 M, unless otherwise defined). When the reduction potential is measured at pH 7, it is represented by the term *E°'*, and the concentration terms in equation 7 can be rearranged to contain only the *formal* concentrations, *F*, of the components of the oxidized and reduced species to give (Harris 2010):

$$E = E°' - \frac{0.05916}{n} \log \left(\frac{F_{oxdized}}{F_{reduced}} \right) \quad (8)$$

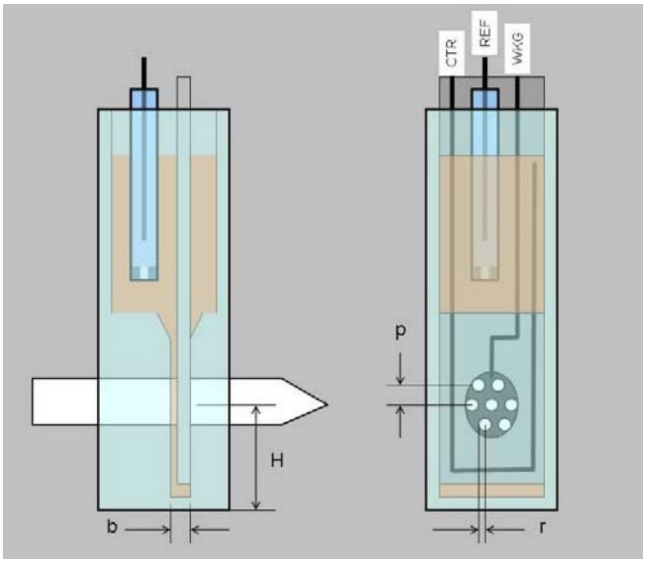

Figure 11. A diagrammatic view of a spectroelectrochemical cell. The working electrode is a gold-coated 19-hole array that allows light (white arrow, side view) to pass through. This is inserted inside a specially designed cuvette. The reference electrode (REF) is placed directly in the solution above the thin channel, and the counter electrode (CTR) flanks the working electrode.

9. Spectroelectrochemistry

Reduction potentials of molecules that have oxidation state-dependent UV-visible spectra can determined by spectroelectrochemistry (SEC), a technique that combines spectroscopy and electrochemistry. This method can be applied to redox pairs such as cytochromes (Figure 8), which have several ideal spectral features within the UV-visible range of the spectrum (~400-650nm). For SEC an optically transparent thin-layer electrode (OTTLE), such as a gold honeycomb electrode (Figure 11) is used to provide a large working electrode surface area within the optical path of the spectrometer. An ideal OTTLE is electrically conductive, chemically inert and has small holes that allow transmission of light. The OTTLE is then inserted into a thin layer quartz cuvette that contains the protein solution. The electrochemical reaction of interest occurs quickly only within an extremely thin layer near the electrode surface, while absorption spectrophotometry requires that light

pass through the entire solution of interest. A chemical species has to diffuse onto the electrode and electron transfer occur on the electrode surface. The ratio of oxidized to reduced species at an applied potential will reach an equilibrium after a period of time. The equilibrium time can be estimated if diffusion is the rate limiting step:

$$\tau=\frac{\delta^2}{D} \quad (9)$$

where τ is the equilibrium time, D is the diffusion coefficient (cm^2/s) and δ is the largest distance a molecule has to travel to the nearest electrode surface. If δ or path length decreases, then equilibrium time decreases, which shortens the duration of experiments.

The reduction potential $E°'$ of a reaction (such as the oxidation-reduction of a cytochrome) is the potential E at which the concentration of oxidized and reduced species are equal. The applied potential of an electrochemical cell is controlled by a potentiostat. Applying a potential at the working electrode or OTTLE using a programmable potentiostat that maintains a constant potential relative to the reference controls the equilibrium of the half-cell reaction. As the applied potential changes, the ratio of oxidized and reduced species changes, which is detected by changes in the UV-visible spectrum. However, the flow of electrons between the working electrode and redox-active species creates a technical problem as current also would also flow through the reference electrode. If too much current flow through the reference electrode occurs its chemical composition could change significantly resulting in inconsistent and inaccurate measurement. To counter this problem, a counter electrode handles the current flow to and from the working electrode that would otherwise be flowing through the reference electrode, thus allowing the reference potential to remain constant.

Examining equation 8, the applied potential has the greatest effect on the ratio of oxidized and reduced species within ±59 mV of the reduction potential, where the concentrations of oxidized and reduced species are within 10% (one log unit) of each other. The relative concentration of the reduced and oxidized species can be ascertained based on the absorbance of a specific peak wavelength relative to the measured absorbance of that peak in the fully oxidized and fully reduced states by following:

$$\frac{[reduced]}{[oxidized]} = \frac{A_{observed}\text{-}A_{reduced}}{A_{oxidized}\text{-}A_{observed}} \quad (10)$$

Substituting equation 9 into equation 8:

$$E_{applied} = E^{\circ\prime} - \frac{0.05916}{n} \log \left(\frac{A_{observed}\text{-}A_{reduced}}{A_{oxidized}\text{-}A_{observed}} \right) \quad (11)$$

By varying the potential incrementally, allowing the solution to reach equilibrium, and plotting the logarithmic term in Equation 11 against the applied potential, a plot such as that in Figure 12 is obtained. Figure 12 shows the results of an SEC experiment on recombinant bovine microsomal cytochrome b_5. This Nernst plot gives a linear regression plot with a slope of 59mV (ideally) and a y-intercept equal to the formal redox potential, $E^{\circ\prime}$ at pH 7, for transfer involving only one electron (n=1).

To accurately measure the absorbance at a given potential, the entire half-cell solution must reach electrochemical equilibrium. This may be impractical as the direct transfer of electrons between the redox protein and the gold working electrode may occur at an extremely low rate. This is the case with cytochromes, as the redox-active centre is buried inside the protein and does not readily transfer electrons even under favourable conditions due to steric hindrance (Bard and Faulkner 2001). This can be at least partially remedied by the inclusion of electron transfer mediators in the protein buffer solution.

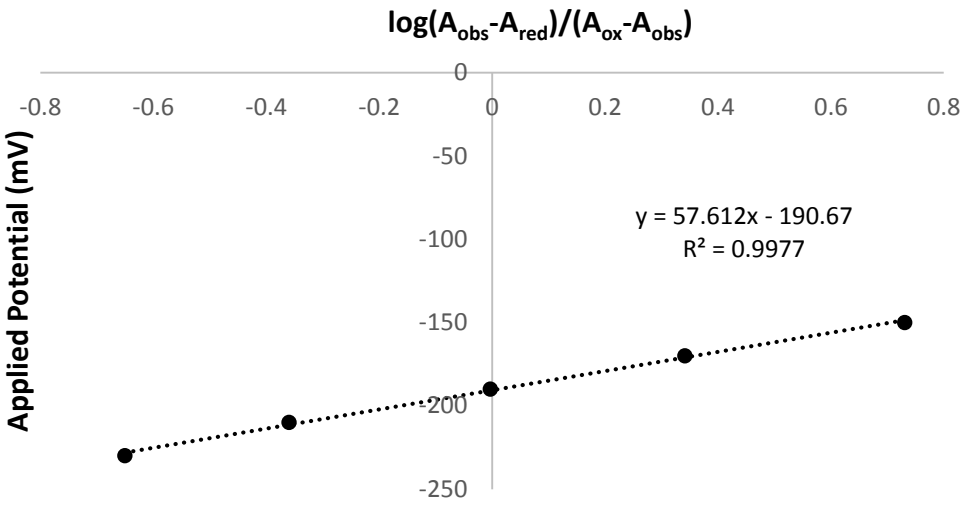

Figure 12. Nernst plot of bovine microsomal cytochrome b_5. The applied potential in millivolts is plotted against the spectroscopically determined ratio of reduced and oxidized bovine microsomal cytochrome b_5 as measured using the 557nm Q-band. Measurements were conducted using the cell pictured in Figure 6. This plot shows a nearly ideal Nernst slope of 57mV with a reduction potential of -190.67 mV (referenced against silver chloride electrode in saturated KCl).

Mediators are typically small organic or transition metal-coordination compounds that readily transfer electrons between the electrode surface and the redox center of proteins hastening the attainment of equilibrium between the working electrode and the protein. In the case of Figure 12, ruthenium hexamine, $Ru(NH_3)_6Cl_3$ was used at a concentration of 0.1mM. Matching the reduction potential of mediators to the expected reduction potential of the redox protein is important for rapid electron transfer. Ideally, mediators should not absorb light in the same wavelength region as the redox active protein and should not react with the protein to alter its reduction potential. Additionally, mediators should have stable oxidized and reduced forms and be soluble in solution at the desired pH.

10. Factors that control the reduction potentials of cytochromes

The reduction potentials of different cytochromes vary considerably and range between -350 mV and +350 mV (all quoted potentials are against the SHE, unless otherwise stated). This spans much of the biochemical range of reduction potentials which lies mainly between -350 mV (NAD^+/NADH) and +820 mV (O_2/H_2O) (Figure 13). As noted in Table 1 the cytochromes b_5, excluding gCYTB5s, occupy a narrower range, yet one that still varies by 180 mV (Figure 13). As all cytochromes b_5 have a pair of histidines as axial ligands, this factor can be excluded from an explanation of their reduction potential differences. Instead, the differences in reduction potential results from orientation of heme within the protein (Walker, Emrick et al. 1988), the hydrophobicity of the heme environment (Mauk and Moore 1997), the electrostatic potential contributed by surface charges (Qian, Wang et al. 2002), accessibility of the heme to solvent (Paoli, Marles-Wright et al. 2002) and heme distortion resulting from steric constraints (Olea, Kuriyan et al. 2010).

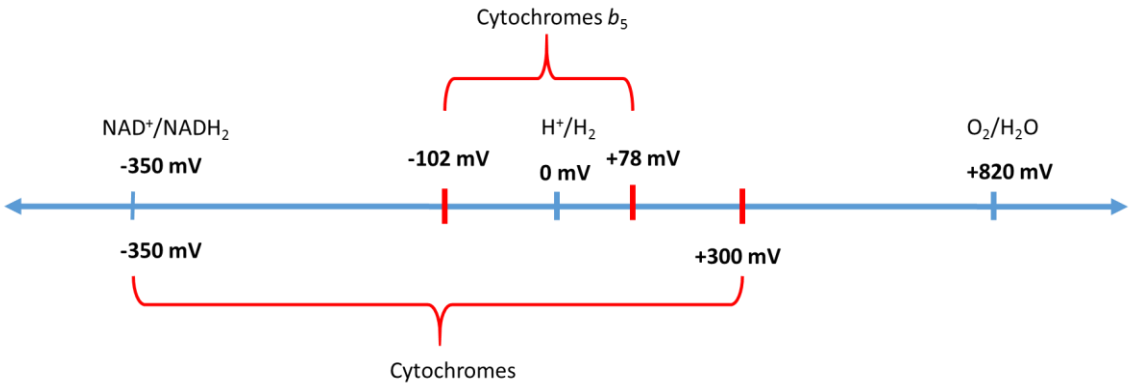

Figure 13. The range of reduction potentials of cytochromes in general and cytochromes b_5 in particular.

11. Thesis aims and approach

The first objective of my thesis is to use spectroelectrochemistry to determine whether gCYTB5- I, -II and -III all have low reduction potentials. As suggested by their homology models, gCYTB5s have more polar heme-binding pockets that their mammalian counterparts, which are predicted to stabilize the oxidized state (Fe^{3+}). Therefore, the second objective is determine if the polarity of these heme-binding pockets contributes to the low reduction potential. To achieve the second objective, I measured the reduction potentials of gCYTB5-I mutants in which candidate polar residues were replaced by non-polar residues that occur in bovine microsomal cytochrome b_5, which has a relatively high reduction potential of +5 mV. The first position, tyrosine-61, is common to all Giardia isotypes. This was mutated to the more hydrophobic phenylalanine residue that occurs in bovine CYTB5A. The second position, tyrosine-51, occurs in gCYTB5-I and –II. This was mutated to phenylalanine, removing the hydroxyl group, and to leucine, which occupies this position in bovine CYTB5A. The third position, cysteine-84, was mutated to phenylalanine as in CYTB5A, and to alanine, which is isosteric with cysteine but lacks the potentially reactive thiol. Furthermore, a triple mutant of the bovine CYTB5A was made to replace three hydrophobic residues with hydrophilic residues found in gCYTB5-I with leucine-25 to tyrosine, phenylalanine-35 to tyrosine, phenylalanine-58 to cysteine. As the biological electron transfer occurs in thermodynamically favorable directions, determining the reduction potentials of gCYTB5s may aid the identification of their redox partners, as well as to comprehend more fully the connection between metalloprotein structure and properties.

MATERIALS AND METHODS

1. Vector preparation

Bacterial expression vectors for bovine CYTB5A, Giardia gCYTB5-I, II, III, gCYTB5-I single mutants and the bovine CYTB5A triple mutant were prepared using the services provided by DNA 2.0 (Menlo Park CA). The coding sequences were codon-optimized for expression in *E. coli* and also encoded N-terminal, tobacco-etch virus (TEV) protease cleavable hexahistidine-tags. These sequences were placed in a pJ401Express vector background, which contains an IPTG-inducible T5 promoter and confers resistance to kanamycin.

2. Expression and purification of recombinant gCYT*b*$_5$s, bovine CYT*b*$_5$ and mutants

Vector pJ401-gCYTB5-I with an N-terminal, TEV-cleavable hexa-histidine-tag was transformed into chemically competent BL21 cells. For each transformation, 1 μL of 5ng/μL of vector was added to 100 μL aliquot of thawed, iced-cold competent cells. The cells were heat-shocked at 42°C and were immediately transferred to 900 μL of LB media in a 15 mL culture tube. The culture was incubated in the shaker at 37°C for 1 hour. Of the cell culture, 100 μL was spread onto a LB+kanamycin (50μg/mL) agar plate and incubated overnight at 37°C. One colony was picked with a sterilized inoculating loop and inoculated in 5 mL of LB+kanamycin (50μg/mL) Broth. The inoculum was incubated at 37°C overnight in the shaker at 220 rpm. This overnight culture was used to inoculate 1 L of Terrific Broth kanamycin (50μg/mL) in a Fernbach flask. The culture was grown at 37°C in the shaker until an OD_{600} of 0.4-0.6 was reached. At this point protein expression was

induced with 1 mM IPTG and the heme precursor δ-aminolevulinic acid 500 μM was also added. The culture was grown overnight at 30 °C in the shaker. Cells were harvested by centrifugation at 16 200 *g* for 30 minutes and the pellet was weighed and stored at -80°C. In parallel, a glycerol cell stock was made by mixing 0.5 mL of the overnight culture with 0.5 mL of 50% glycerol. This was stored at -80°C and was used as the source of inoculum for future cultures. The above procedure was repeated for gCYTB5 -II, -III; gCYTB5-I mutants Tyr51→Phe, Tyr51→Leu, Tyr61→Phe, Cys84→Ala, Cys84→Phe; bovine CYTB5A and CYTB5A triple mutant Leu25→Tyr-Phe35→Tyr-Phe58→Cys vectors.

The cell pellet was thawed at room temperature and resuspended in 10 volumes (v/w) of Thermo Scientific Pierce B-PER reagent in 46 mM sodium phosphate buffer, pH 7.0 with 1 mM TCEP (reducing agent) and 1 mM of each protease inhibitors PMSF and captopril. The cell suspension was incubated at room temperature for 30 minutes. 2.5 mM magnesium chloride, 0.5 mM calcium chloride and 0.01 mg/mL of DNase I was added to lower the viscosity of the lysate caused by the release of bacterial DNA. The cell suspension was centrifuged at 15 000 *g* for 20 minutes to separate soluble proteins (including the cytochrome) from the insoluble proteins and cell debris. The presence of the cytochrome was detected by bright-red colour of the supernatant. The supernatant was decanted and was brought to 20% (w/v) ammonium sulfate saturation followed by gentle stirring for 40 minutes at 4 °C. The solution was centrifuged at 15 000 *g* for 20 minutes and the pellet was discarded. The supernatant was brought to 60% (w/v) saturation with ammonium sulfate to precipitate cytochrome b_5. The solution was centrifuged as before, the supernatant discarded and the red pellet was retained for the next step.

The cytochrome was purified by immobilized metal affinity chromatography,

taking advantage of the affinity of the polyhistidine tag for the resin. A 2 mL His-Pur column charged with Co^{2+} (Thermo Scientific Pierce) was prepared by passing through 20 mL of equilibration buffer (50 mM sodium phosphate, 300 mM sodium chloride, 1 mM imidazole at pH 7.4) at a flow rate of 5 mL/min using a peristaltic pump. The ammonium sulfate pellet containing the cytochrome was resuspended in 10 mL of equilibration buffer and applied to the column at a flow rate of 1 mL/min such that the total volume loaded did not exceed 200 mg of protein. Since the cytochrome is red, a reddish band was detected at the top of the column as the loading progressed, indicating binding of the cytochrome to the resin. After the protein was loaded, the column was washed with 2 column volumes of wash buffer (50 mM sodium phosphate, 300 mM sodium chloride, 10 mM imidazole, pH 7.4) at flow rate of 2 mL per minute. The protein was eluted with 20 mL of elution buffer (50 mM sodium phosphate, 300 mM sodium chloride, 500 mM imidazole at pH 7.4) at flow rate of 1 mL per minute. A Bio-Gel P-6DG desalting column 3 cm by 23 cm (*w x l*) (Bio-Rad Canada, Mississauga) was used to exchange the eluted protein into ionic strength (μ) = 0.1 M (47 mM) sodium phosphate, pH 7.0 buffer. The desalting column was equilibrated with 2 column volumes of this buffer. Before application to the column a few grains of ferricyanide were added to the cytochrome solution to ensure full oxidation of the protein and to act as a low-molecular weight marker. (Imidazole is colourless and ferricyanide is orange. Since imidazole and ferricyanide have small molecular weight, they co-elute much later on the size exclusion column and ferricyanide can be detected by the naked eye. The cytochrome is larger and elutes earlier). The desalted protein was concentrated by ultrafiltration using Amicon® Ultra 15 mL Centrifugal filters (10,000 molecular weight cut-off) at 3000 *g* for 20 minutes.

3. Sodium Dodecyl Sulfate Polyacrylamide Gel Electrophoresis (SDS-PAGE)

The protein sample for SDS-PAGE was prepared by mixing 2 μL of desalted protein, 8 μL of water and 3.75 μL of 4X sample loading buffer. The sample was heated at 70 °C for 5 minutes, centrifuged in a microcentrifuge at 5000 *g* for 1 minute then loaded onto a 14% SDS-PAGE gel. The gel tank was filled with 1X Tris-Glycine buffer and electrophoresis was done at 150 V for 1 hour and 15 minutes. The gel was stained with Coomassie Brilliant Blue dye using a microwave protocol and was destained overnight in water.

4. UV-Visible spectroscopy of cytochromes b_5

The oxidized and reduced spectra of cytochrome b_5 were obtained on a Cary 400 Bio UV-visible spectrophotometer (Figure 10). The baseline was first recorded by scanning a buffer blank such as a solution of ionic strength (μ) of 0.1 M sodium phosphate, pH 7.0 in a 1 mL quartz cuvette from 250 nm to 700 nm. Cytochrome b_5 was pipetted into the cuvette and an oxidized spectrum was recorded using the Cary 400 in scanning mode. To obtain the reduced spectrum, a few granules of sodium dithionite was added to the cuvette. (The half reaction for sodium dithionite reduction is:

$2SO_3^{2-} + 2H_2O + 2e^- \rightarrow S_2O_4^{2-} + 4OH^-$ $E° = -1.12$ V (12)

Where dithionite, $S_2O_4^{2-}$, is oxidized and SO_3^{2-} is reduced).

5. Quantification of cytochrome b_5 protein

The concentrations of purified solutions of cytochromes were determined by Bradford Assay. Using, bovine serum albumin (BSA) as the standard. A 0.10 mg/mL stock

solution of BSA was used to make 1.2 mL standards with 0, 2, 4, 6, 8, 10, 12, 14, 16, 18 and 20 μg each of BSA in 1.0 mL Bradford Dye Reagent and water. Duplicates of each standard was made. The Cary 400 Bio UV-visible spectrophotometer was first zeroed at 595 nm with the blank standard in a polymethyl methacrylate disposable plastic cuvette (Sigma Aldrich Canada, Oakville ON) and the absorbance of each standard in increasing concentration was recorded. A standard curve was prepared by plotting A_{595} versus mass of protein in μg. Samples of cytochrome b_5 were prepared by mixing 100 μL of diluted protein, 100 μL of water and 1 mL of Bradford reagent. The absorbance of protein sample was recorded and only when the absorbance was within the range of the standard curve, was the concentration of the protein determined.

6. Pyridine hemochrome assay

To determine the heme content of the purified cytochrome, 0.5 mL of cytochrome b_5 with an estimated protein concentration of 0.5 mg/mL was mixed with an equal volume of freshly prepared Reagent A (0.2 mL of 5 M sodium hydroxide, 2.5 mL of pyridine and water for a final volume of 5 mL) in a quartz cuvette. A few granules of solid sodium dithionite was added to this mixture to reduce the heme. The spectrum of the reduced pyridine hemochrome complex was recorded from 250 nm to 700 nm on a Cary 400 Bio UV-visible spectrophotometer against a baseline of buffer and Reagent A. Heme concentrations were calculated based on the difference in absorbance at 556 nm (peak) and 540 nm (trough) using an absorption coefficient of 22.1 $mM^{-1}cm^{-1}$.

7. Spectroelectrochemistry

All of the apparatus was obtained from Pine Research, Durham NC. The electrode card contained a built-in honeycomb working electrode with gold-plated channels (125 μm hole radius) and a patterned counter electrode adjacent to the working electrode (Figure 11). The reference electrode (3.5 mm diameter, 60 mm length) was an Ag/AgCl type in saturated KCl gel with a ceramic fitted tip (197 mV vs SHE). A special cuvette cap was used to hold the electrode card and the reference electrode in a quartz slotted thin-layer cell (1.7 mm optical path length) (Figure 14). The electrode card and the reference electrode were connected *via* a mini-USB cable to a Wave Now portable USB potentiostat/galvanostat (Figure 15). The applied potential was controlled by a laptop using AfterMath Instrument Control and Data Analysis Software. Prior to each experiment, the quartz cell was cleaned with chromic acid by soaking for 30 minutes, the electrode card was cleaned by soaking in 15 mL of a 3:1(v/v) sulfuric acid and 30% hydrogen peroxide solution for 30 minutes and the reference electrode was cleaned with saturated KCl solution.

The quartz cell was filled with 1 mL of μ=0.1 M sodium phosphate pH 7.0. The electrode card and the reference electrode were inserted into the cuvette cap, and this assembly was placed into the cell holder of the Cary 400 Bio UV-Visible spectrophotometer. A baseline from 200 nm to 700 nm was recorded in the Cary Scan program. Once the baseline was collected, the solution was replaced with 600 μL of 0.2-0.5 mM of cytochrome b_5 in buffer containing the redox mediators, ruthenium hexamine, 2-hydroxy-1, 4-naphthoquinone, and methylviologen (Sigma-Aldrich Canada, Oakville ON). A layer of silicone oil (100 μL) was pipetted to the top of the protein solution to prevent evaporation. The cell was constantly flushed with a gentle stream of argon

throughout the experiment to prevent autoxidation.

The honeycomb and the reference electrodes were then connected to the potentiostat and a spectrum was obtained without any applied potential. The potential was then set at -600 mV vs Ag/AgCl until the protein was fully reduced. To follow this electrochemical reduction, the absorbance of the reduced cytochrome b_5 band at 557 nm was recorded until the absorbance value was stable indicating that protein sample was fully reduced. The reduced spectra was then recorded. Subsequently the applied potential was increased stepwise to -400 mV and the process was repeated until the protein was fully oxidized (Figure 16). As the ratio of oxidized to reduced species is most sensitive to applied potentials within 59 mV of the reduction potential, the step size within this expected range was 20 mV rather than the 100 mV step used outside this range. The applied potential and the change in absorbance is plotted to generate the Nernst plot (Figure 12). The reduction potential measured against the Ag/AgCl reference is then converted to the standard reduction potential vs SHE by addition of 197 mV. Due to the extended duration of protein SEC experiments (typically >6hrs), oxygen must also be purged from the cell to prevent auto-oxidation of the cytochrome, this is accomplished by a constant influx of argon or other inert gas into the cell headspace, displacing oxygen.

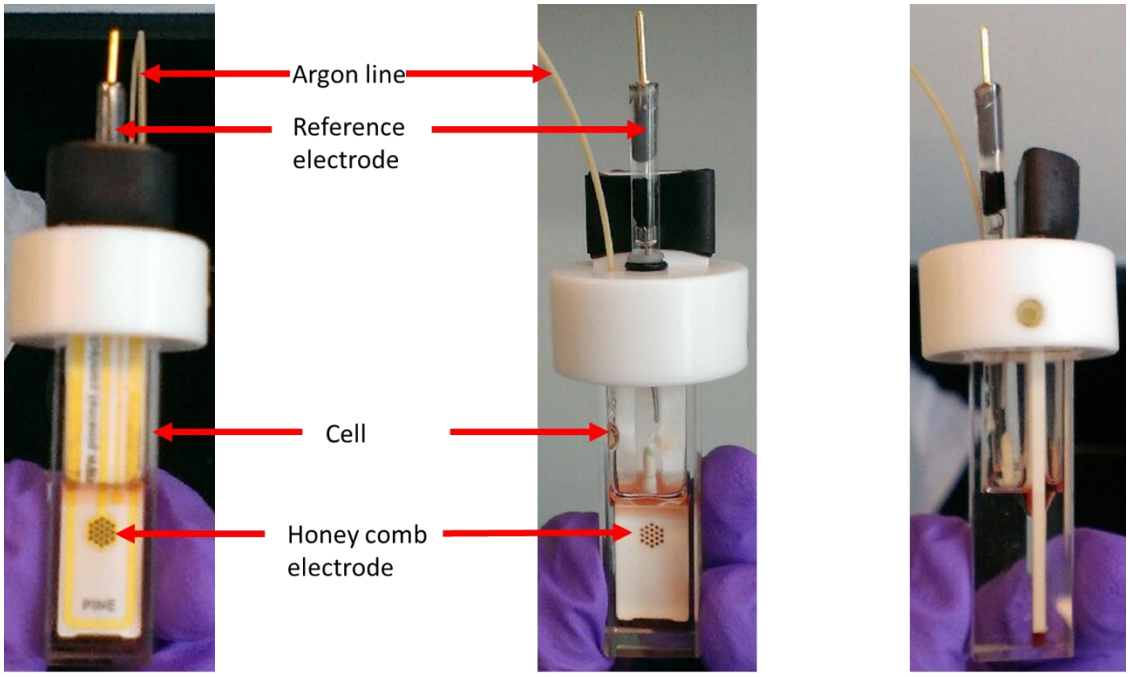

Figure 14. **Spectroelectrochemical cell assembly.** Quartz cell, honeycomb electrode, argon line and reference electrode,. Note the red colour of the solution that contains the cytcohrome and the mediators.

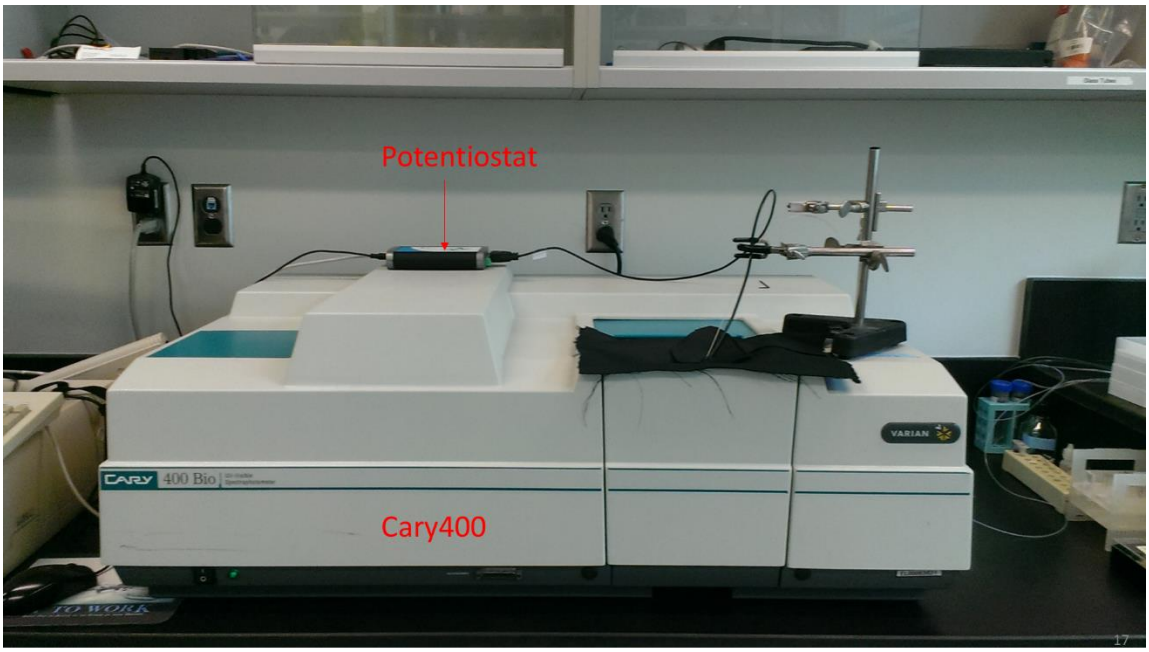

Figure 15. Final spectroelectrochemistry setup. The cell is placed into the Cary 400 UV-visible spectrophotometer while a potential is applied by the WaveNow potentiostat, controlled by a laptop, not shown (Pine Research, Durham NC).

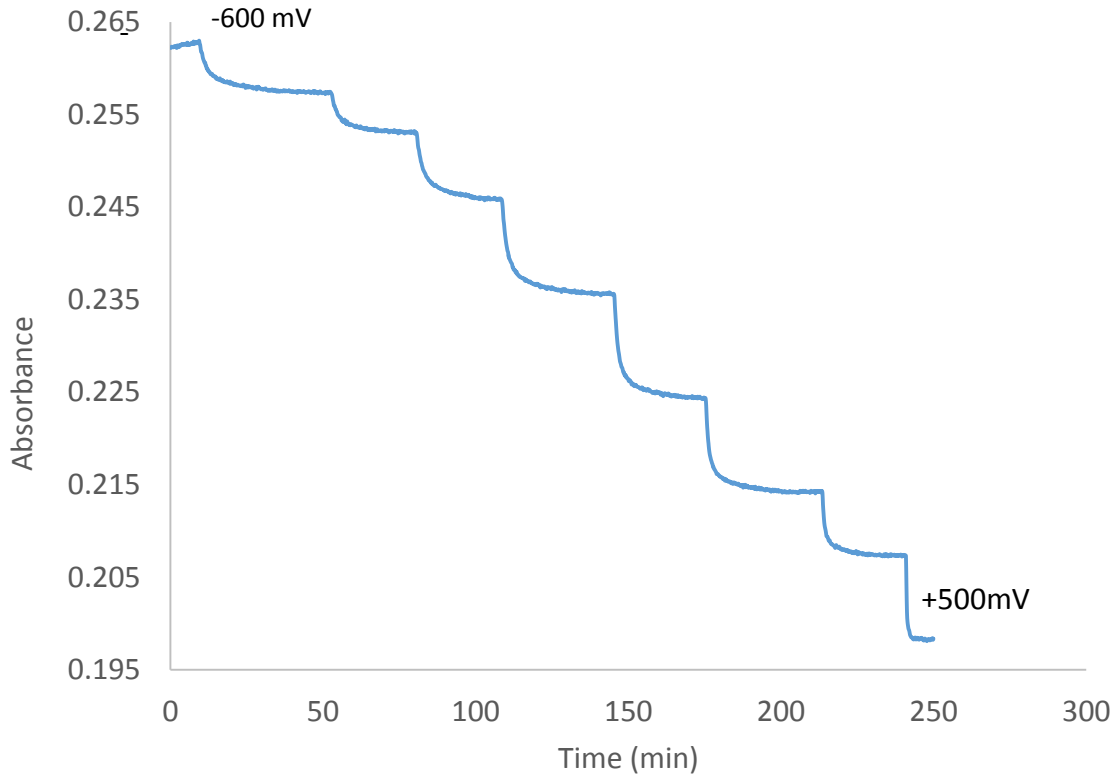

Figure 16. A sample electrochemical experiment. CARY 400 kinetic trace of Giardia cytochrome b_5 I C84A mutant from -600mv to +500mv. The absorbance at 557 nm was recorded over time as the applied potential changed from -600 mV (fully reduced) to +500 (fully oxidized). The largest change in absorbance occurs within ±59 mV of the reduction potential.

RESULTS

The cytochromes differ somewhat in chain length such that analogous positions will have different amino acid numbers in different proteins. To make comparisons easier, the corresponding analogous residues in bovine CYTB5A and gCYTB5s are cross-referenced in Table 2:

Table 2. Corresponding amino acid residues in bovine CYB5A and gCYTB5s

Bovine CYB5A	**gCYTB5-I (*mutants*)**	**gCYTB5-II**	**gCYTB5-III**
Leu25	Tyr51 (*Leu, Phe*)	Tyr53	His52
Phe35	Tyr61 (*Phe*)	Tyr63	Tyr62
His39	His64	His67	His66
Phe58	Cys84 (*Phe, Ala*)	Ala86	Thr85
His63	His88	His90	His89

1. UV-visible spectroscopy

The UV-visible spectra of recombinant bovine CYTB5A agree well with those observed by others (Strittmatter 1960), with an intense Soret band (γ) at 413 nm and 423 nm in the oxidized and reduced states respectively (Figure 17). The spectra of gCYTB5 isotypes and gCYTB5-I mutants resemble those of bovine CYTB5A, with slight differences in the positions of peaks (Figure 18 and Table 3). Collectively these spectra are those expected for bis-histidyl heme complexes that remain low spin in both the oxidized and reduced states.

The bovine CYTB5A triple mutant resembles the parent wild type but differs in two significant ways. While it has similar spectroscopic features as the wild type, it also has an

additional absorbance band at 660 nm, which is associated with a change in the colour of the oxidized cytochrome from red to brown (Figure 19). This is consistent with a fraction of the heme existing in a high spin state. Second, the extent of heme incorporation, as measured by the pyridine hemochrome assay is only 15%, whereas wild type and single amino acid site mutants are typically obtained with at least 60% of the protein containing heme (Alam, Yee et al. 2012)

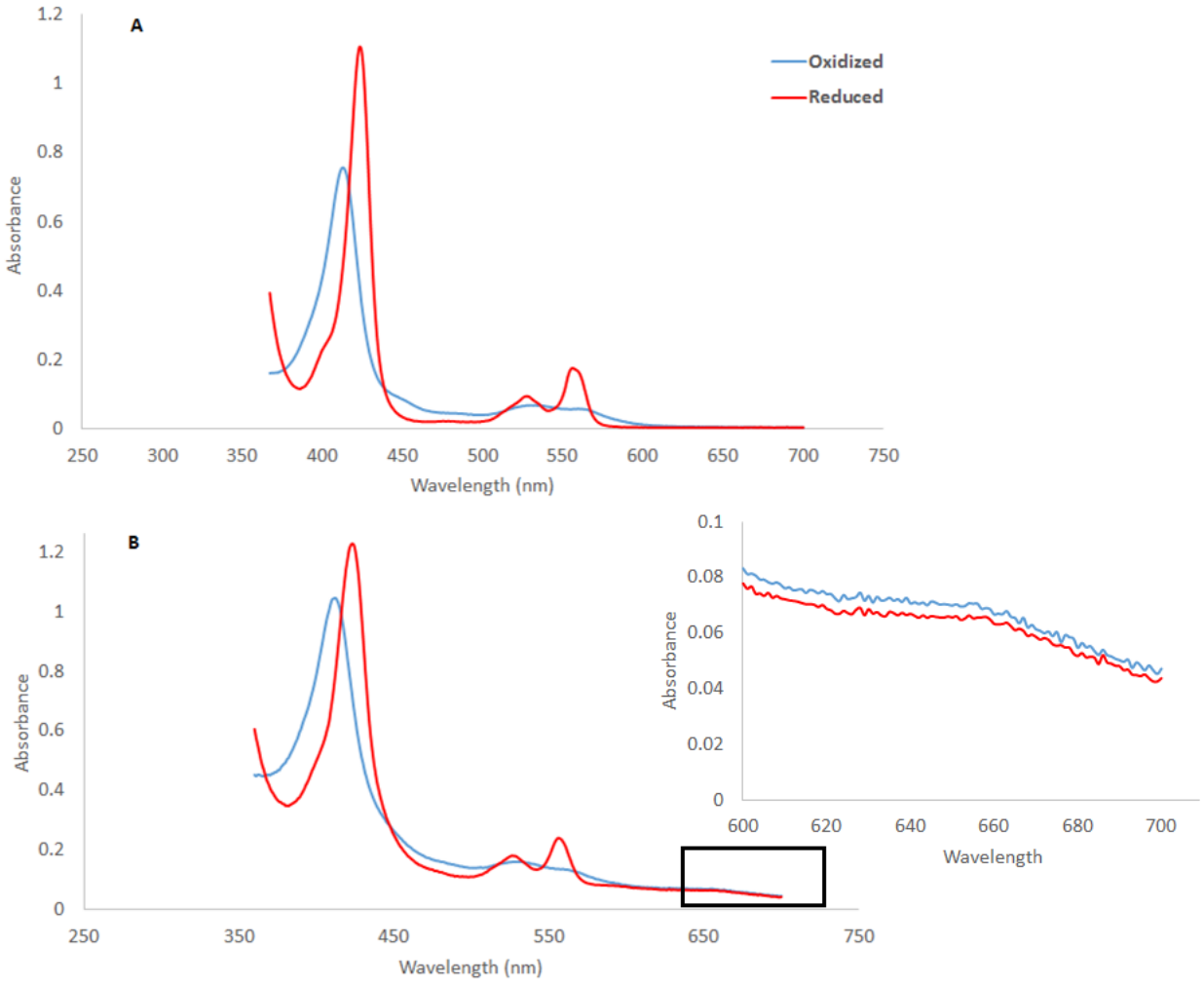

Figure 17. **The UV-Visible spectra of A) bovine microsomal cytochrome *b*$_5$ and B) bovine microsomal cytochrome *b*$_5$ triple mutant (Leu25Tyr, Phe35Tyr, and Phe58Cys).** In the oxidized heme state, the spectra of both protein displayed a Soret peak at 413 nm (triple mutant) and 414 nm (bovine wild type). In the reduced heme state, the spectra of both protein displayed a shift in the Soret peak (423nm) and presence of alpha (527nm) and beta (556nm) peaks. Bovine triple mutant had a shoulder in the 660 nm region indicated by the black box and magnified. Absorbance in the 660 nm empirically indicates high spin heme.

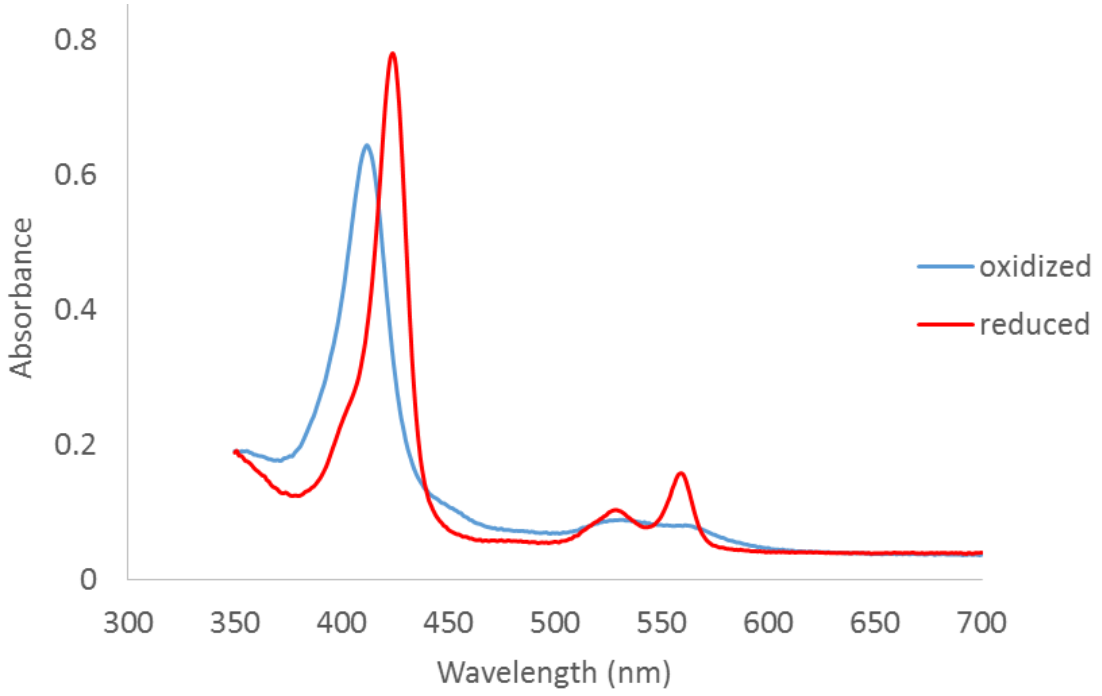

Figure 18. The UV-Visible spectra of Giardia cytochrome b_5-I Cys84Ala mutant in oxidized and reduced state. The UV-visible spectra of Giardia cytochrome b_5-I mutants resemble the UV-Visible spectra of Giardia cytochrome b_5 isotypes and other cytochrome b_5 members. The typical Soret peak at 410 nm in oxidized state. The Soret band shifts to 423 nm and presence of alpha (α) peak at 527 nm and beta (β) peak at 556 nm is indicated in the reduced state.

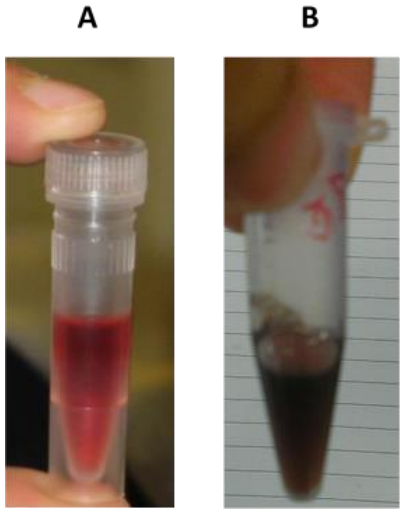

Figure 19. **Purified fractions of A) bovine microsomal cytochrome b_5 and B) bovine microsomal cytochrome b_5 triple mutant.** Bovine microsomal cytochrome b_5 and Giardia cytochrome b_5 isotypes are red. Bovine microsomal cytochrome b_5 triple mutant is brown.

2. Spectroelectrochemistry

The length of each spectroelectrochemical experiment lasts between 8 to 10 hours, with the initial full reduction of the protein taking from 90 minutes to three hours. From the fully-reduced state the applied potential is increased in a stepwise manner; each step takes between 20 to 40 minutes to reach equilibrium with one or two mediators (Figure 16). The temperature of each experiment was monitored with a thermometer placed within the chamber of the spectrophotometer. While temperature was not actively controlled, the ambient temperature over the course of each experiment varied no more than 0.5 degree from 22 °C. At this temperature the expected slope of the Nernst plot is 58 mV. Experiments in which the Nernst slope was greater than 66mV were not used, but were repeated.

The reduction potential of bovine CYTB5A was +7 mV vs SHE which matches well with a reported value of +5 mV measured by the same method (Reid, Taniguchi et al. 1982). The reduction potentials of all three gCYTB5s isotypes are considerably lower than this, with values of -171 mV, -140 mV, and -157 mV for gCYTb5 I, II and III respectively (Table 3 and 4).

Table 3. Reduction potential measurements. Bold indicates wild type (native) data.

Protein	**λ_{max}, nm**	**E°', mV vs SHE**
CYTb5, bovine microsomal	Oxidized: 413 Reduced: 423, 527, 556	**+7 ±0.745**
CYTb5, bovine microsomal, L25Y-F35Y-F58C	Oxidized: 414 Reduced: 423, 527, 556	-128 ± 0.710
gCYTB5-I, wild type	Oxidized: 411 Reduced: 423, 528, 558	**-171 ± 1.50**
gCYTB5-I, Y61F	Oxidized: 410 Reduced: 422, 528, 558	-73 ± 1.11
gCYTB5-I, Y51F	Oxidized: 412 Reduced: 420, 527, 560	-148 ± 0.708
gCYTB5-I, Y51L	Oxidized: 410 Reduced: 419, 527, 559	-153 ± 0.481
gCYTB5-I, C84A	Oxidized: 412 Reduced: 423, 530, 559	-114 ± 0.103
gCYTB5-I, C84F	Oxidized: 411 Reduced: 424, 531, 560	-136 ± 0.953
gCYTB5-II, wild type	Oxidized: 410 Reduced: 419, 525, 554	**-140 ± 3.44**
gCYTB5-III, wild type	Oxidized: 410 Reduced: 425, 530, 559	**-157 ± 0.719**

Table 4. A comparison of reduction potential of cytochrome b_5 from different species. The reduction potential was determined using spectroelectrochemistry. Mc and OM are microsomal and mitochondrial outer membrane cytochrome b_5, respectively.

Source organism	**Potential (mV vs SHE)**	**Electrode**	**Mediators**	**References**
bovine Mc	5.1±0.1	gold	$Ru(NH3)_6^{2+/3+}$ (12 μM)	(Reid *et al.* 1982)
rat OM	-102±2	gold minigrid	$Ru(NH3)_6^{2+/3+}$ (0.4 mM) methyl viologen (1 mM)	(Rivera, Wells et al. 1994)
human testis OM	-40	gold	100 μM of $[Ru(NH_3)_6]Cl_3$ and methyl viologen	(Altuve, Wang et al. 2004)

To determine the reason for these low potentials, we performed spectroelectrochemical experiments on heme pocket mutants of gCYTB5-I**.** As the numbering of analogous residues differs among the cytochromes owing to differences in chain length, a correlation table is provided for the reader's convenience that cross-references these positions (Table 2). The replacement of hydrophilic amino acid residues in the heme pocket of gCYTB5-I with the hydrophobic residues in found in analogous positions in bovine CYTB5A increases the reduction potential of these variants, as did isosteric mutations that did not alter the shape of the residue significantly but increased the hydrophobicity (Table 3). Of the three positions examined, substitutions at gCYTB5-I position-61 exhibited the largest change, with an increase in reduction potential of 98 mV when tyrosine-61 was replaced with phenylalanine. Position-51 was least susceptible to changes in reduction potential, with increases of about 25 mV, while substitutions at position-84 had intermediate effects.

As a complement to the mutagenic experiments on gCYTB5-I to make its heme

pocket more hydrophobic as in bovine CYTB5A, we also mutated bovine CYTB5A to resemble that of gCYTB5-I by introducing all three polar substitutions at once: Leu25→Tyr, Phe35→Tyr, and Phe58→Cys. The reduction potential of this bovine triple mutant was -128 mV, thereby decreasing the reduction potential -135 mV. However, as noted above the level of heme incorporation in this mutant was poor. Furthermore the Nernstian slope obtain from its spectroelectrochemical experiment was 85 which is not the ideal slope of 59 for one electron transfer reaction (Table 5). This suggests that apart from lowering the reduction potential the mutations in CYTB5A destabilize the protein fold such that it cannot bind heme well, and that its electrochemical behavior is not completely reversible.

Table 5. The Nernstian slope and *E*°' (y-intercept) vs. SHE for bovine cytochrome b_5, Giardia cytochrome b_5 and mutants. The measurements are from independent experiments using spectroelectrochemistry. The most accurate reduction potential is in bold.

Protein	**Exp. No.**	**λ (nm)**	**Nernst slope**	***E*°' vs. SHE (mV)**	**Applied E range (mV vs. Ag/AgCl)**
Bovine microsomal	**1**	**557**	**60 ±1.82**	**+7 ±0.745**	**-500 mV to +500 mV**
Bovine triple mutant	1	557	96	-148	-500 mV to +500 mV
	2	**557**	**84 ±2.13**	**-128 ±0.710**	**-500 mV to +500 mV**
gCYTB5-I, wild type	1	557	145	-242	-500 mV to +500 mV
	2	557	98	-266	-500 mV to +500 mV
	3	557	86	-200	-500 mV to +500 mV
	4	**557**	**62 ±2.31**	**-171 ±1.50**	**-500 mV to +500 mV**
	5	557	112	-208	-500 mV to +500 mV
gCYTB5-I, Y61F	1	557	186	-139	-500 mV to +500 mV
	2	557	69	-77	-500 mV to +500 mV
	3	**557**	**66 ±1.11**	**-73 ±1.11**	**-500 mV to +500 mV**
gCYTB5-I, Y51F	**1**	**557**	**66 ±0.708**	**-148 ±0.708**	**-500 mV to +500 mV**
	2	557	98	-205	-500 mV to +500 mV
gCYTB5-I, Y51L	1	557	68	-145	-600 mV to +500 mV
	2	**557**	**67 ±0.481**	**-153 ±0.817**	**-600 mV to +500 mV**
gCYTB5-I, C84A	1	557	118	-192	-600 mV to +500 mV
	2	**557**	**64 ±0.103**	**-114 ±0.102**	**-600 mV to +500 mV**
gCYTB5-I, C84F	1	557	85	-151	-600 mV to +500 mV
	2	**557**	**63 ±1.37**	**-136 ±0.953**	**-600 mV to +500 mV**
gCYTB5-II, wild type	**1**	**557**	**62 ±8.21**	**-140 ±3.44**	**-500 mV to +500 mV**
gCYTB5-III, wild type	**1**	**557**	**62 ±1.89**	**-157 ±0.719**	**-500 mV to +500 mV**

DISCUSSION

1. Experimental sources of error

One issue was the length of time that was needed to fully reduced cytochrome b_5. Over the course of these experiments, which generally last about 10 hours, evaporation of water from the solution can occur, especially as the sample was being flushed with a stream of argon over this time. Solvent evaporation alters the concentration of the solution and can also cause protein precipitation, which can impede spectroscopic measurements or cause loss of electrical conductivity if the circuit is broken. To avoid solvent evaporation an additional hole (Figure 20) was drilled into the electrochemical cell cap to apply a layer silicone oil on the smaller side of the gold electrode. This allowed a small layer of silicon oil to blanket entirely the top of the solution.

A second issue was baseline drift in the absorbance values. Even after three hours of applying a potential of -600 mV, the absorbance continued to increase slightly. The reduction potential is calculated based on the absorbance of a specific peak relative to the measured absorbance of that peak in the fully oxidized and fully reduced form:

$$E_{\text{half cell}} = E^{\circ} + \frac{RT}{nF} \ln \frac{[\text{A}_{\text{oxidized}}]}{[\text{A}_{\text{reduced}}]} \quad (7)$$

Consequently, if the absorbance of the fully reduced form is not accurate, the calculation of the formal reduction potential and Nernst slope will be affected.

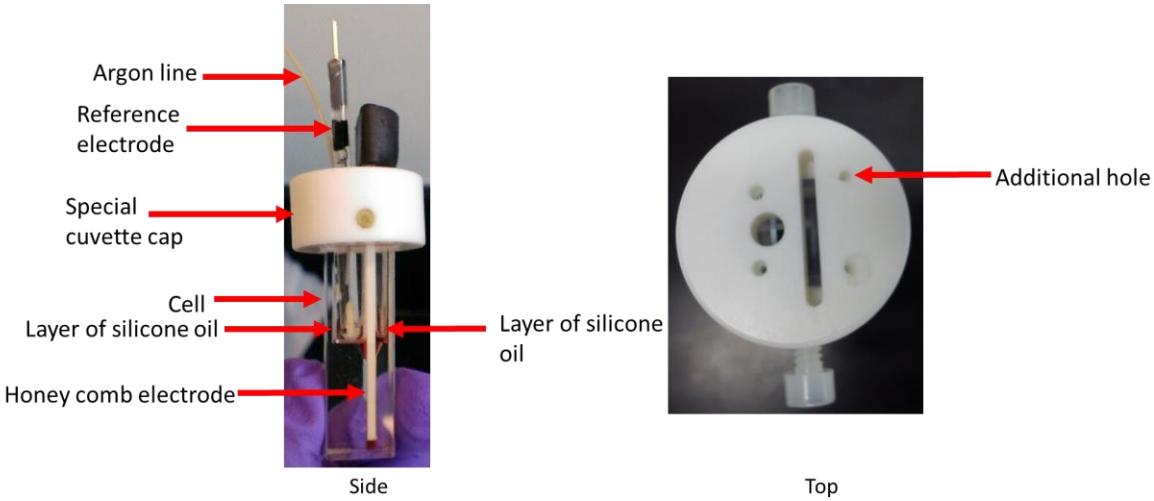

Figure 20. **Side and top view of the modified spectroelectrochemical cell set up.** An additional hole was drilled into the special cuvette cap to ensure a layer of silicon oil on both sides of the honey comb electrode to prevent buffer evaporation.

2. UV-Visible spectroscopy

With one exception all of the proteins have spectra that are expected for cytochromes b_5 that are characteristic of low spin six-coordinate complexes with a pair of histidine residues. These defining features are i) a Soret peak at 410 – 413 nm in the oxidized state that shifts to 420 – 423 nm upon reduction ii) α and β bands near 560 nm and 530 nm respectively in the reduced state. While the UV-visible spectra of the bovine triple mutant is similar to that of the wild type, the additional shoulder at 660 nm is a unique feature, and suggests that this protein is in equilibrium with a high-spin state species with loss of one of the histidine residues. For example, the oxygen storage heme protein myoglobin also has a shoulder in the 650 nm region (Figure 21) which is consistent with a high spin ferric heme complex (Fe^{3+}). The structure of myoglobin in this state is shows that the iron is coordinated by a single histidine ligand with water as the sixth ligand (Evans and Brayer 1990). In the triple mutant of CYTB5A, due to three amino acid substitutions, the heme-binding core may have gone under significant conformational changes such that

one of the axial histidines no longer coordinates the iron and a water molecule may serve as the sixth ligand (Li and Mabrouk 2003). It is likely that histidine 63 (Figure 27) is the labile ligand, as two of the three amino acid substitutions are closest to this residue. Substitution of leucine-25 and phenylalanine-58 with tyrosine and cysteine respectively could have changed the protein conformation such that histidine-63 is no longer in a position to donate its electrons to the iron centre. The change in coordination would explain the absorbance shoulder in the 660 nm region.

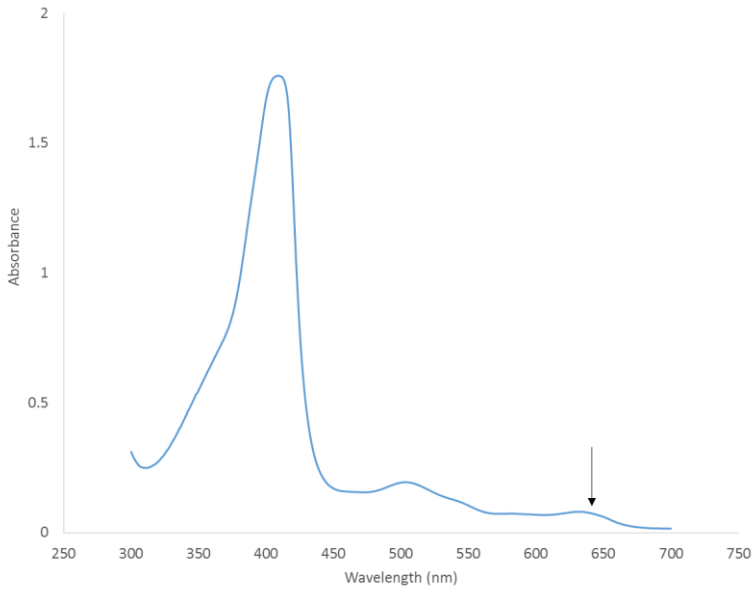

Figure 21. **The UV-Visible spectra of oxidized myoglobin**. The Soret peak is at 409 nm and a shoulder is at 644 nm indicating high-spin heme.

3. Reduction potentials of gCYTB5 variants

We measure a reduction potential for bovine CYB5A of +7 mV which agrees well with a value of +5 mV (Reid, Taniguchi et al. 1982) which was also obtained by spectroelectrochemistry. The reduction potential of gCYTB5-I, II and III all were significantly lower than bovine CYTB5A, the lowest being that of gCYTB5-I (-171 mV vs

SHE). Based on their similar UV-visible spectra all of these share the same set of axial ligands, thus variation in the identity of the ligands can be excluded as the basis for this difference. Beyond the nature of the axial ligands a major factor that influences the reduction potential of heme proteins is the polarity of the heme binding pocket. As noted in the introduction, when the iron (Fe^{2+}) coordinated by heme loses an electron, the iron becomes oxidized (Fe^{3+}). The porphyrin ring itself has a negative two charge; therefore, the overall net charge becomes +1 when iron loses an electron. Conversely, when iron is reduced (Fe^{2+}) the overall net charge on heme is zero. Based on these considerations the reduced state is favored in a more nonpolar environment and the oxidized state in a more polar one. The heme-binding pocket of bovine CYTB5A is lined with highly conserved nonpolar residues such as Phe58, Leu23, Leu46, Leu30, Leu36 and Phe74, which help to stabilize the reduced form of heme (Lederer 1994). Non-polar residues favour the reduced state because they cannot stabilize charge. When the heme environment favours the reduced form of heme, thereby gaining an electron, the reduction potential increases as the case in bovine CYTB5A.

In contrast, the heme-binding pockets of the Giardia cytochromes includes more polar amino acid residues than bovine CYTB5A. Interestingly all of the gCYTB5s have in common a tyrosine residue at the position corresponding to phenylalanine 35 in bovine CYTB5A, namely tyrosine 61, 63 and 62 in gCYTB5-I, II and III respectively. Homology model of all three isotypes show that the phenol ring of this tyrosine is in a similar position and orientation as the phenyl ring of phenylalanine 35 in bovine CYTB5A. However, the hydroxyl group of tyrosine would be directed towards the plane of the heme within van der Waals contact of the cofactor, which may explain the lower reduction potentials of all three

gCYTB5s that were measured (Figure 22). The significance of the nature of this particular residue in controlling the reduction potential is also supported by previous spectroelectrochemical studies by others on bovine CYTB5A in which mutation of phenylalanine 35 to tyrosine lowers the reduction potential from +2 mV to -64 mV due to increased stabilization of the oxidized state (Yao, Xie et al. 1997). Moreover, the cytochrome b_5 domain of human NADH-cytochrome b_5 oxidoreductase (Ncb5or), which shares ~35% sequence identity with gCYTB5s also has a tyrosine the corresponding position 35 in bovine CYTB5A; it too has a low reduction potential of -108 mV (Deng, Parthasarathy et al. 2010). Our measurements on the Tyr61→Phe mutant of gCYTb5-I, discussed below, provide direct support that this residue is significant in explaining much of the low reduction potential of the Giardia proteins.

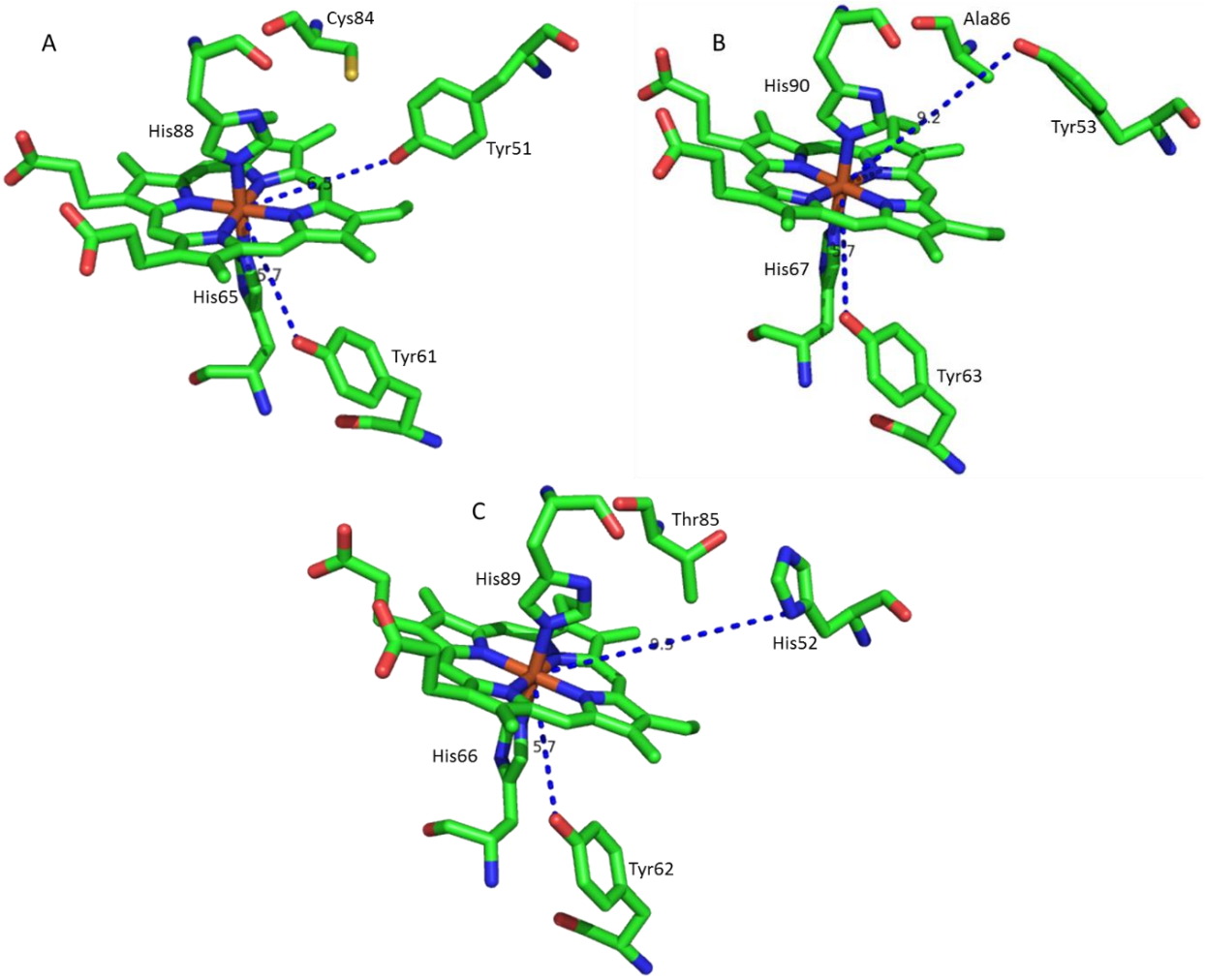

Figure 22. **Homology model of heme binding site of Giardia cytochromes b_5 isotype A) I, B) II, C) III.** Tyrosine 61, 63, and 62 are at the same distance of 5.7 Å and conformation from the heme co-factor. The hydrophilic residues help to stabilize the oxidized heme; therefore, decreasing the reduction potential.

Comparing the reduction potential of Giardia isotypes, isotype I has the lowest reduction potential, followed by isotype III (-157 mV vs SHE) and II (-140 mV vs SHE). Isotype I has cysteine 84 instead of phenylalanine 58 found in bovine CYTB5A, which interacts with the imidazole ring of histidine 63 in a face-to-face π-stacking mode and with the porphyrin ring of the heme (Shan, Lu et al. 2005). These stacking interactions are absent in the Giardia isotypes I, II and III because there is no aromatic side chain in cysteine,

alanine, and threonine that replaces phenylalanine respectively. Cys84 of gCYTB5-I has a thiol group that has a polarizable sulfur atom positioned above the porphyrin ring that may help to stabilize iron in the oxidized state (Figure 22). Isotype II has an alanine residue (Ala86) which is of the same size as cysteine but lacks its polarizable sulfur atom, which may explain its higher reduction potential compared to gCYTB5-I. The influence of cysteine 84 was explored by characterizing the gCYTB5-I Cys84→Ala mutation and the reduction increased when alanine was substituted for cysteine. Isotype III has a threonine residue at this position (Thr85). Although the hydroxyl group of the threonine is polar, and this residue would be expected to lower the reduction potential if placed near the heme, the oxygen atom of the hydroxyl group is smaller than sulfur of the thiol; its electrons are closer to its nucleus and therefore the alcohol is less easily polarizable than the thiol of cysteine. Consequently, the threonine residue at this position may have less influence over the reduction potential compared to cysteine, explaining in part the relatively higher reduction potential of gCYTB5-III over gCYTB5-I. Alternatively, the orientation of the threonine side chain may direct its methyl group rather than the hydroxyl group towards the heme.

At the residue corresponding to bovine CYTB5A position Leu25, gCYTB5-I and II have a tyrosine residue (Tyr51 in isotype-I; Tyr53 in isotype-II) while gCYTB5-III has histidine (His52). Leu25 lies on the same side of the heme as the second of the two histidine ligands near the back of the heme pocket, with the side chain directed towards the cofactor. All three side chains in the Giardia proteins are planar, polar, and capable of hydrogen bonding whereas Leu25 has a branched alkyl side chain. Interestingly, while both gCYTB5-I and II have tyrosine at this position the side chains in the model structures adopt difference conformations owing to rotation about the Cα-Cβ bond (Figure 23). The

hydroxyl group of Tyr51 in gCYTB5-I directly point towards the porphyrin ring (6.5 Å away) in a conformation similar to Leu25 of bovine CYTB5A. The hydroxyl group can stabilize the iron in the oxidized state (Fe^{3+}), thereby decreasing the reduction potential. However, the side chain of Tyr53 in gCYTB5-II and of His52 in gCYTB5-III point away from the porphyrin ring and are further away from the heme (9.2 Å) compared to tyrosine 51 (6.5 Å) in isotype I shown in the homology models (Figure 23). The molecular graphics program PyMOL permits some manual modification of the position of the side chains in the structural files of the proteins. When the conformation of Tyr53 in gCYTB5-II was changed to match that of Tyr51 in gCYTB5-I, severe steric clash with adjacent residues was encountered. Whether these residues truly adopt different conformations will only be known when the actual structures (rather than homology models) are solved.

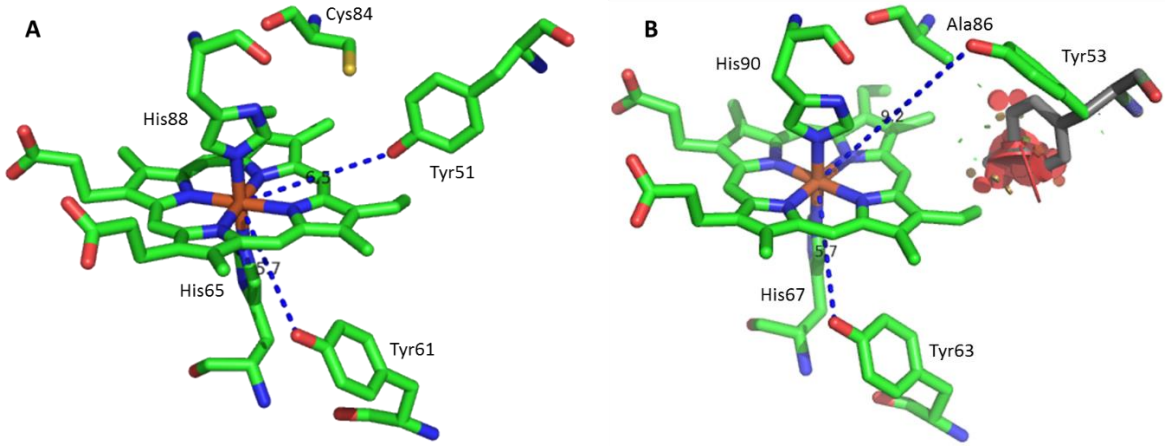

Figure 23. **Homology model of heme binding site of gCYTB5-I (A) and gCYTB5-II (B).** Both have a tyrosine residue at position 51 and 53 respectively; however, in isotype II, the conformation of tyrosine 53 residue points away from the heme cofactor at a distance of 9.2 Å compared to tyrosine 51 that points toward the heme cofactor at a distance of 6.5 Å. Tyrosine 51 in isotype I may be able to stabilize the oxidized heme more effectively, resulting in a lower reduction potential. If tyrosine 53 of gCYTB5-II was placed in the same conformation as tyrosine 51 in gCYTB5-I, steric clashing (red patches) results, suggesting that structural rearrangement in this region of the protein likely occurs.

Overall, the relatively polar heme-binding pocket in the Giardia cytochromes favors the oxidized iron state compared to bovine CYTB5A. The presence of a tyrosine residue

in all isotypes at the same position within van der Waals contact of the heme (Tyr61, Tyr63 and Tyr63, in isotypes I, II, and III respectively) strongly suggests that this residue makes a significant contribution to their low reduction potentials. Yet it is difficult to say with certainty which residues are most important, owing to sequence variation among the three isotypes studied. For this reason, a set of single-site mutants in gCYTB5-I were then characterized. By varying a single residue at a time the contribution of each position to the redox potential could be assessed with greater precision.

4. Reduction potential of gCYTB5-I variants

To identify the quantitative effect of the nature of the amino acid residues at gCYTB5-I positions-61, 84, and 51 on reduction potential, these three amino acids were replaced with the non-polar amino acid residues found in bovine CYTB5A (Tyr61→Phe, Cys84→Phe, Tyr51→Leu), plus two other isosteric mutations that decreased the polarity of the side chain without significantly changing its shape (Cys84→Ala, Tyr51→Phe). All mutants had higher reduction potentials than wild type gCYTB5-I (-171 mV), and of these Tyr61→Phe (Figure 24) had the highest reduction potential (-73 mV) (Table 2). This confirmed our hypothesis that this position, of the three tested, contributes the most to the

low potentials observed for the Giardia cytochromes.

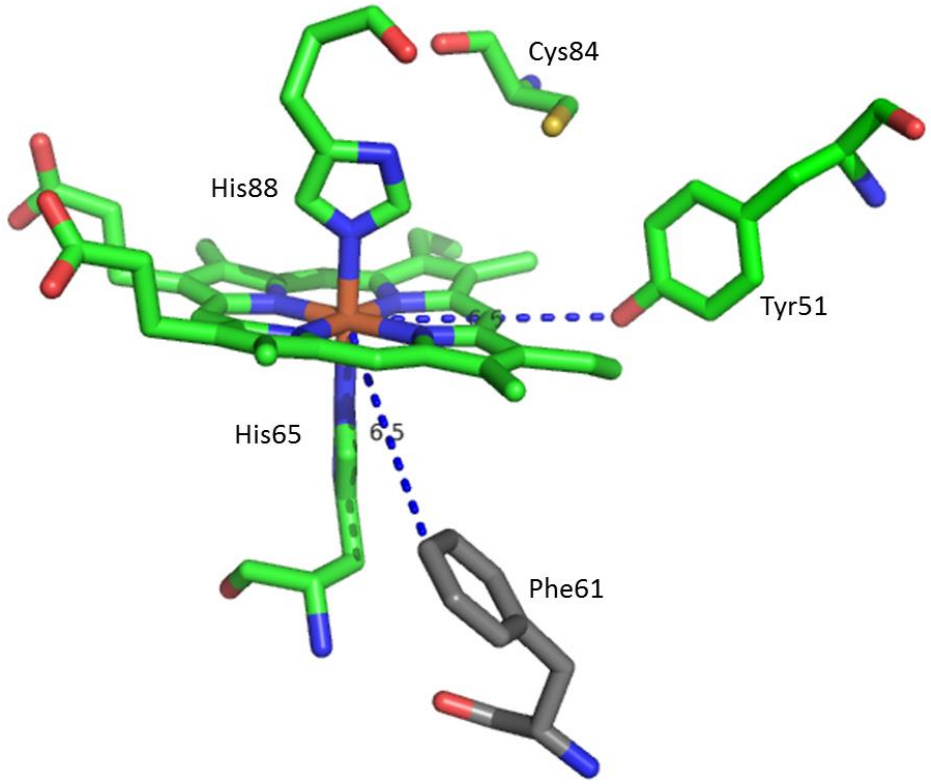

Figure 24. **Homology model of heme binding site of Giardia cytochrome b_5 isotype I Y61F mutant.** Removal of the hydroxyl group on tyrosine 61 to phenylalanine increased the reduction potential 88 mV. Mutant Y61F had the highest reduction potential (-73 mV) of all single mutants and isotype I (-177 mV).

Interestingly the Cys84→Ala (Figure 25) variant also has a substantial effect on the reduction potential, raising it by 63 mV to -114 mV, suggesting that the electronegative sulfur atom of the cysteine side chain is also important in stabilizing the oxidized heme in gCYTB5-I. The other variant at this position, gCYTB5-I Cys84→Phe (Figure 25), has the third highest reduction potential (-136 mV). While its reduction potential is higher than the wild type protein, one would expect that it would be higher than Cys84→Phe, as it is more hydrophobic than alanine, and a phenylalanine occurs at this position in bovine

CYTB5A. However, the introduction of a large residue to replace a smaller one likely causes adjacent residues to shift in conformation to accommodate the phenyl ring, which may shift other polar residues closer to the heme cofactor or increase the exposure of the heme to solvent. However, this is speculation and solving the structure of these variants by X-ray crystallography would provide a definitive answer.

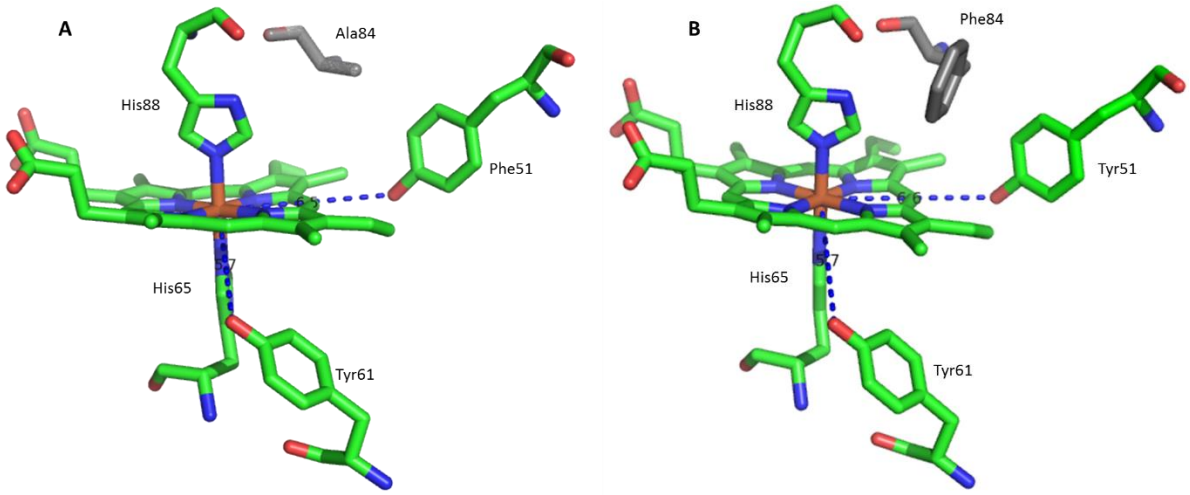

Figure 25. **Homology model of heme binding site of Giardia cytochrome b_5 isotype I A) C84A and B) C84F mutant.** C84A had the second highest reduction potential (-114 mV vs SHE). The reduction potential increased by 63 mV compared to isotype I. C84F had the third highest reduction potential of -136 mV.

Replacement of the tyrosine at position-51 of gCYTB5-I by more hydrophobic residues increased the reduction potential but not to the same extent as similar substitutions at position 61 and 84. gCYTB5-I variants Tyr51→Phe and Tyr51→Leu have similar reduction potentials of -148 mV and -153 mV respectively. One reason could be that the phenylalanine and leucine residue (Figure 26) are further away from the heme (7.2 and 8.4 Å respectively) and thus have less impact on the reduction potential. Tyrosine 51 (Figure 26) in the wild type gCYTB5-I had less impact on the reduction potential because it was

9.2 Å away from the heme compared to tyrosine 61 at 6.5 Å.

Overall, the single mutants show that changing the immediate heme environment to a more hydrophobic surrounding increases the reduction potential, especially at position-61 and position-84. Substitutions at position-51 to non-polar residues also increased the reduction potential, but to a lesser extent possible due to a greater distance from the heme group.

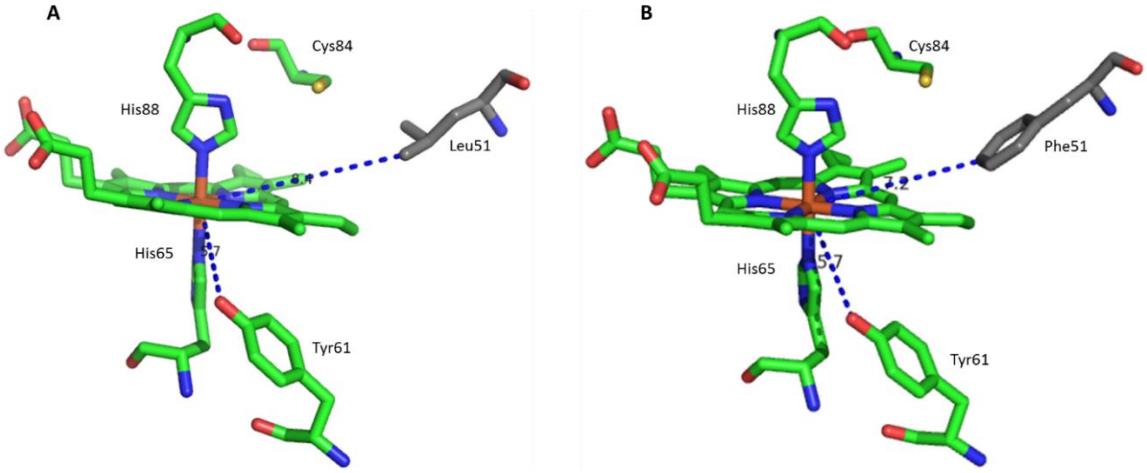

Figure 26. **Homology model of heme binding site of Giardia cytochrome b_5 isotype I A) Y51L and B) Y51F mutant.** Y51F had the fourth highest reduction potential (-148 mV vs SHE). Y51L had the third highest reduction potential of -153 mV vs SHE.

5. Reduction potential of bovine CYTB5A and CYTB5A triple mutant

The studies on mutants of gCYTB5-I indicate that the low reduction potentials of the Giardia cytochromes are due to more polar heme environments. This suggests that the reduction potential of bovine CYTB5A would decrease if its heme environment were made more polar as well. A previous experiment showed that the bovine CYTB5A Phe35→Tyr mutant had a reduction potential of -66 mV, which is 73 mV lower than wild type (Yao,

Xie et al. 1997) . To extend this further a triple mutant of bovine CYTB5A was made such that the three non-polar residues were replaced by the three polar residues that occur in gCYTB5-I (Leu25→Tyr, Phe35→Tyr, Phe58→Cys) (Figure 27). The reduction potential of this triple mutant was -128 mV compared to the wild type of +7 mV and consistent with an increased polarity of the heme environment. However, the Nernst slope of 85 for this bovine CYTB5A triple mutant deviates significantly from the expected slope of 58 for reversible transfer of a single electron between two redox-active states at 22°C, so the its reduction potential may not be accurate. The large Nernst slope the unique shoulder in 660 nm in the UV-visible spectra, and the brown colour of the protein suggest that the heme environment has changed significantly. In particular the shoulder in the 660 nm likely indicates the presence of high spin heme, suggesting that a fraction of the protein is five-coordinate or six-coordinate with a weak field ligand such as water replacing one of the histidine ligands. A previous mutagenesis study showed that the bovine CYTB5A His63→Met variant was high spin penta-coordinate and could bind exogenous ligands such as carbon monoxide in the reduced state (Bodman, Schuler et al. 1986). It is possible that due to the three amino acid substitutions, one of the axial histidine ligands no longer coordinates the heme and it may be replaced by water. Loss of a histidine ligand would also be expected to weaken heme binding, and indeed we observed that the level of heme incorporation in the triple mutant based on the pyridine hemochrome assay, is only 15%, whereas wild type and single amino acid site mutants are typically obtained with at least 60% of the protein containing heme (Alam, Yee et al. 2012). Having four possible states of the CYTB5A triple mutant that vary in oxidation and spin state may also explains the deviation the expected slope in the Nernst plot.

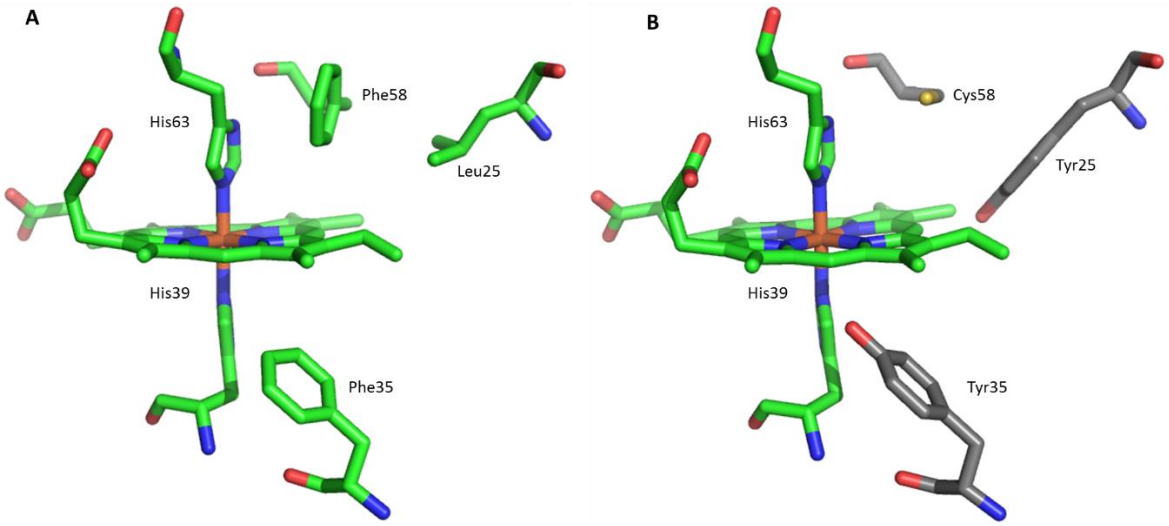

Figure 27. **Heme binding site of A) bovine microsomal cytochrome b_5 and B) homology model of the bovine microsomal cytochrome b_5 triple mutant.** The reduction potential of bovine triple mutant was -128 mV vs SHE compared to the wild type of +7 mV vs SHE. However, the Nernst slope of the triple mutant was 85 which is above the accepted slope of 59 for one electron transfer at 25°C.

6. Functional implications of the electrochemical properties of gCYTB5s

The biochemical roles of gCYTB5s in Giardia have not been identified. However, knowing the reduction potential of each isotype gives provides information on some of the likely properties of its redox partners. As electron transfer proteins gain an electron from a donor that has a lower reduction potential and transfers the electron to an acceptor of higher reduction potential, knowing the reduction potential of Giardia isotypes can give a rough estimate of the reduction potential of their redox partners. Since gCYTB5s have low reduction potential (-171 mV to -140 mV) compared to other family members with higher reduction potentials (~0 mV for bovine CYTB5A, for example), the Giardia proteins may have entirely different partners. Giardia possesses the flavoenzyme GiOR1, a cytochrome P450 oxidoreductase (POR) homologue that efficiently reduces gCYTB5-I, III and IV (gCYTB5 II was not evaluated) (Pyrih, Harant et al. 2014). The fact that GiOR1 can reduce at least three different gCYTB5 isotypes indicates that a specific electron donor for each

cytochrome may not be necessary, which is similar to the ability of human POR to donate electrons to multiple cytochrome P450 isotypes (Pandey and Fluck 2013). However, GiOR1 has both flavin adenine dinucleotide (FAD) and flavin mononucleotide (FMN) cofactors, it seems overly complex to act solely in this role, as known NAD(P)H cytochrome b_5 oxidoreductases require only a single flavin cofactor, not two (Bewley, Marohnic et al. 2001). In eukaryotes POR and cytochrome b_5 both participate in cytochrome P450 monooxygenation reactions, POR as an electron donor and cytochrome b_5 as an electron shuttle between POR and P450, or as a modulator of the activity of the latter (Schenkman and Jansson 2003). Since Giardia has GiOR1, a POR homologue and cytochrome b_5, it might also possess cytochrome P450s, but none have been identified within its genome. The degree of sequence identity across the cytochrome P450 family can be as low as 10% may present as a challenge, but nearly half of the open reading frames of the Giardia genome are annotated as hypothetical proteins, which leaves open the possibility that a Giardia P450 awaits discovery.

7. Future experiments

The most important experiments that could be done that are relevant to this work are structural studies on the Giardia cytochromes either by X-ray diffraction or NMR spectroscopy to confirm the observations made in homology models. Furthermore, to establish the roles of these proteins the redox partners of gCYTB5s could be identified using pull-down assays. Our recombinant gCYTB5s can be bound to a metal affinity resin through their hexahistidine tags to act as bait to bind prospective partners in cell Giardia lysates. This may also require chemical crosslinking as interactions between redox partners, while highly specific, are often transient. If successful, the redox partner-cytochrome b_5

covalent complex could be detected by a shifted band on the SDS-PAGE, which could be excised and further analysed by mass spectrometry to identify the partner. Such experiments are ongoing in the lab.

Conclusions

Despite lacking a mitochondria and heme biosynthetic pathway *Giardia intestinalis*, an aerotolerant anaerobic parasite produce five heme proteins: four cytochromes b_5 and one flavohemoglobin. gCYTB5s have approximately 38% sequence identity to other members of the cytochrome b_5 family and have typical UV-Visible spectra features common to the cytochrome b_5 family. However, gCYTB5-I, II and III have reduction potentials that are more than 100 mV lower than other family members such as the well-studied bovine CYTB5A. A major factor that contributes to their low reduction potential is the polar nature of the heme-binding pocket, which was confirmed by the properties of gCYTB5-I mutants that had nonpolar substitutions in the heme pocket and higher reduction potentials. Conversely, replacement of three nonpolar residues in CYTB5A with polar ones greatly lowered its reduction potential, although at the expense of the stability of heme binding.

The functions and redox partners of gCYTB5-I, -II,-III are still unknown. Determining the reduction potential can elucidate its redox partners as electron transfer occur from a donor with a lower reduction potential to an acceptor with a higher reduction potential. The presence of four cytochromes b_5 in Giardia suggest possible new metabolic pathways and the unique properties of gCYTB5-I, -II,-III make them an interesting addition to the cytochrome b_5 family.

REFERENCES

Ajioka, R. S., J. D. Phillips and J. P. Kushner (2006). "Biosynthesis of heme in mammals." Biochim Biophys Acta **1763**(7): 723-736.

Alam, S. (2014). Expression and characterization of cytochrome b_5 from *Giardia lamblia*. Msc, Trent University.

Alam, S., J. Yee, M. Couture, S. J. Takayama, W. H. Tseng, A. G. Mauk and S. Rafferty (2012). "Cytochrome b_5 from *Giardia lamblia*." Metallomics **4**(12): 1255-1261.

Altuve, A., L. Wang, D. Benson and M. Rivera (2004). "Mammalian mitochondrial and microsomal cytochromes b_5 exhibit divergent structural and biophysical characteristics." Biochemical and Biophysical Research Communications **314**(2): 602-609.

Ankarklev, J., J. Jerlstrom-Hultqvist, E. Ringqvist, K. Troell and S. G. Svard (2010). "Behind the smile: cell biology and disease mechanisms of Giardia species." Nat Rev Microbiol **8**(6): 413-422.

Bard, A. and L. Faulkner (2001). Spectroelectrochemistry and other coupled characterization methods: In: Electrochemical methods: Fundamentals and applications. New York, Wiley and Sons.

Bewley, M. C., C. C. Marohnic and M. J. Barber (2001). "The structure and biochemistry of NADH-dependent cytochrome b_5 reductase are now consistent." Biochemistry **40**(45): 13574-13582.

Bodman, S. B. V., M. A. Schuler, D. R. Jollie and S. G. Sligar (1986). "Synthesis, bacterial expression, and mutagenesis of the gene coding for mammalian cytochrome b_5." Proc. Natl. Acad. Sci. USA **83**: 9443-9447.

Brown, D. M., J. A. Upcroft, M. R. Edwards and P. Upcroft (1998). "Anaerobic bacterial metabolism in the ancient eukaryote *Giardia duodenalis*." Int J Parasitol **28**(1): 149-164.

Deng, B., S. Parthasarathy, W. Wang, B. R. Gibney, K. P. Battaile, S. Lovell, D. R. Benson and H. Zhu (2010). "Study of the individual cytochrome b_5 and cytochrome b_5 reductase domains of Ncb5or reveals a unique heme pocket and a possible role of the CS domain." J Biol Chem **285**(39): 30181-30191.

Evans, S. V. and G. D. Brayer (1990). "High-resolution study of the three-dimensional structure of horse heart metmyoglobin." J Mol Biol **213**(4): 885-897.

Eyring, H. (1935). "The Activated Complex and the Absolute Rate of Chemical Reactions." Chem. Rev **17**(1): 65–77.

Funk, W. D., T. P. Lo, M. R. Mauk, G. D. Brayer, R. T. A. MacGillivray and A. G. Mauk (1990). "Mutagenic, electrochemical, and crystallographic investigation of the

cytochrome b5 oxidation-reduction equilibrium: involvement of asparagine-57, serine-64, and heme propionate-7." Biochemistry **29**(23): 5500-5508.

Guiard, B. and F. Lederer (1977). "The "b_5-like" domain from chicken-liver sulfite oxidase: a new case of common ancestral origin with liver cytochrome b_5 and bakers' yeast cytochrome b_2 core." Eur J Biochem **74**(1): 181-190.

Harris, D. C. (2010). Quantitative chemical analysis. New York, W.H. Freeman and Co.
Holler, D., F. Skoog and S. Crounch (2007). Introduction to Ultraviolet-Visible Molecular Absorption Spectrometry. In: Principles of Instrumental Analysis. Boston.

Ito, A., S. Hayashi and T. Yoshida (1981). "Participation of a cytochrome b_5-like hemoprotein of outer mitochondrial membrane (OM cytochrome b) in NADH-semidehydroascorbic acid reductase activity of rat liver." Biochem Biophys Res Commun **101**(2): 591-598.

Jagow, G. (1980). "*b*-type cytochromes." Annual Review of Biochemistry **49**: 33.
Jian Han, L. J. C. (2012). "Reconstruction of Sugar Metabolic Pathways of *Giardia lamblia*." International Journal of Proteomics **2012**: 9.

Lederer, F. (1994). "The cytochrome b_5-fold: an adaptable module." Biochimie **76**(7): 674-692.

Li, Q. C. and P. A. Mabrouk (2003). "Spectroscopic and electrochemical studies of horse myoglobin in dimethyl sulfoxide." Journal of Biological Inorganic Chemistry **8**(1-2): 83-94.

Lindmark, D. G. (1980). "Energy metabolism of the anaerobic protozoon *Giardia lamblia*." Mol Biochem Parasitol **1**(1): 1-12.

Lippard, S. and M. J. Berg (1994). Principles of Bioinorganic Chemistry. United States of America, University Science Books.

Mathews, F. S., M. Levine and P. Argos (1971). "The structure of calf liver cytochrome b_5 at 2.8 A resolution." Nat New Biol **233**(35): 15-16.

Mauk, A. G. and G. R. Moore (1997). "Control of metalloprotein redox potentials: What does site-directed mutagenesis of hemoproteins tell us?" Journal of Biological Inorganic Chemistry **2**(1): 119-125.

Mitoma, J. Y. and A. Ito (1992). "The Carboxy-Terminal 10-Amino Acid Residues of Cytochrome-b_5 Are Necessary for Its Targeting to the Endoplasmic-Reticulum." Embo Journal **11**(11): 4197-4203.

Morrison, H. G., A. G. McArthur, F. D. Gillin, S. B. Aley, R. D. Adam, G. J. Olsen, A. A. Best, W. Z. Cande, F. Chen, M. J. Cipriano, B. J. Davids, S. C. Dawson, H. G. Elmendorf, A. B. Hehl, M. E. Holder, S. M. Huse, U. U. Kim, E. Lasek-Nesselquist, G.

Manning, A. Nigam, J. E. J. Nixon, D. Palm, N. E. Passamaneck, A. Prabhu, C. I. Reich, D. S. Reiner, J. Samuelson, S. G. Svard and M. L. Sogin (2007). "Genomic Minimalism in the Early Diverging Intestinal Parasite Giardia lamblia." Science **317**: 1921-1926.

Ogishima, T., J. Y. Kinoshita, F. Mitani, M. Suematsu and A. Ito (2003). "Identification of outer mitochondrial membrane cytochrome b_5 as a modulator for androgen synthesis in Leydig cells." J Biol Chem **278**(23): 21204-21211.

Olea, C., J. Kuriyan and M. A. Marletta (2010). "Modulating Heme Redox Potential through Protein-Induced Porphyrin Distortion." Journal of the American Chemical Society **132**(37): 12794-12795.

Pandey, A. V. and C. E. Fluck (2013). "NADPH P450 oxidoreductase: structure, function, and pathology of diseases." Pharmacol Ther **138**: 229-254.

Paoli, M., J. Marles-Wright and A. Smith (2002). "Structure-function relationships in hemeproteins." DNA and Cell biology **21**(4): 271–280.

Paul, K., H. Theorell and A. Akenson (1953). "The molar light absorption of pyridine ferroprotoporphyrin (pyridine hemochromagen)." Acta Chem. Scand **7**.

Petragnani, N., O. C. Nogueira and I. Raw (1959). "Methaemoglobin reduction through cytochrome b_5." Nature **184(Suppl 21)**: 1651.

Pyrih, J., K. Harant, E. Martincova, R. Sutak, E. Lesuisse, I. Hrdy and J. Tachezy (2014). "*Giardia intestinalis* incorporates heme into cytosolic cytochrome b_5." Eukaryot Cell **13**(2): 231-239.

Qian, W., Y. H. Wang, W. H. Wang, P. Yao, J. H. Zhuang, Y. Xie and Z. X. Huang (2002). "Redox properties of cytochrome b_5: a mutagenesis and DPV study of the pH and ionic strength dependence of redox potentials and interactions with myoglobin by DPV." Journal of Electroanalytical Chemistry **535**(1-2): 85-96.

Rafferty, S., B. Luu, R. E. March and J. Yee (2010). "*Giardia lamblia* encodes a functional flavohemoglobin." Biochem Biophys Res Commun **399**(3): 347-351.

Reid, L., V. Taniguchi, H. Gray and G. Mauk (1982). "Oxidation-Reduction Equilibrium of Cytochrome b_5." J. Am. Chem. SOC **104**: 7516-7519.

Reid, L. S. and A. G. Mauk (1982). "Kinetics analysis of cytochrome b5 reduction by (ethylenediaminetetraacetato)ferrate(2-) ion." Journal of the American Chemical Society **104**(3): 841-845.

Rivera, M., M. A. Wells and F. A. Walker (1994). "Cation-promoted cyclic voltammetry of recombinant rat outer mitochondrial membrane cytochrome b_5 at a gold electrode modified with beta-mercaptopropionic acid." Biochemistry **33**(8): 2161-2170.

Savioli, L., H. Smith and A. Thompson (2006). "Giardia and Cryptosporidium join the 'Neglected Diseases Initiative'." Trends Parasitol. **22**(5): 203-208.

Schenkman, J. B. and I. Jansson (2003). "The many roles of cytochrome b_5." Pharmacol Ther **97**(2): 139-152.

Sergeev, G. V., A. A. Gilep, R. W. Estabrook and S. A. Usanov (2006). "Expression of outer mitochondrial membrane cytochrome b_5 in *Escherichia coli*. Purification of the recombinant protein and studies of its interaction with electron-transfer partners." Biochemistry-Moscow **71**(7): 790-799.

Shan, L., J. X. Lu, J. H. Gan, Y. H. Wang, Z. X. Huang and Z. X. Xia (2005). "Structure of the F58W mutant of cytochrome b_5: the mutation leads to multiple conformations and weakens stacking interactions." Acta Crystallogr D Biol Crystallogr **61**(Pt 2): 180-189.

Sigel, H. (1991). Electron Transfer Reactions in Metalloproteins. Metal Ions in Biological Systems. New York, Marcel Dekker.

Smith, L. J., A. Kahraman and J. M. Thornton (2010). "Heme proteins--diversity in structural characteristics, function, and folding." Proteins **78**(10): 2349-2368.

Vergeres, G. and L. Waskell (1995). "Cytochrome b_5, its functions, structure and membrane topology." Biochimie **77**(7-8): 604-620.

Walker, F. A., D. Emrick, J. E. Rivera, B. J. Hanquet and D. H. Buttlaire (1988). "Effect of heme orientation on the reduction potential of cytochrome b_5." J Am Chem Soc **110**(18): 6234-6240.

Yao, P., Y. Xie, Y. H. Wang, Y. L. Sun, Z. X. Huang, G. T. Xiao and S. D. Wang (1997). "Importance of a conserved phenylalanine-35 of cytochrome b_5 to the protein's stability and redox potential." Protein Eng **10**(5): 575-581.